Towards UAV-based MEC Service Chain Resilience Evaluation: A Quantitative Modeling Approach

Jing Bai, Xiaolin Chang, Ricardo J. Rodríguez, Kishor S. Trivedi, Shupan Li

***Abstract*—Unmanned aerial vehicle (UAV) and network function virtualization (NFV) facilitate the deployment of multi-access edge computing (MEC). In the UAV-based MEC (UMEC) network, virtualized network function (VNF) can be implemented as a lightweight container running on UMEC host operating system (OS). However, UMEC network is vulnerable to attack, which can result in resource degradation and even UMEC service disruption. Rejuvenation techniques, such as failover technique and live container migration technique, can mitigate the impact of resource degradation but their effectiveness to improve the resilience of UMEC services should be evaluated. This paper presents a quantitative modeling approach based on semi-Markov process to investigate the resilience of a UMEC service chain consisting of any number of VNFs executed in any number of UMEC hosts in terms of availability and reliability. Unlike existing studies, the semi-Markov model constructed in this paper can capture the time-dependent behaviors between VNFs, between host OSes, and between VNFs and host OSes on the condition that the holding times of the recovery and failure events follow any kind of distribution. We perform the sensitivity analysis to identify potential resilience bottlenecks. The results highlight that migration time is the parameter significantly affecting the resilience, which shed the insight on designing the UMEC service chain with high-grade resilience requirements. In addition, we carry out the numerical experiments to reveal that: (i) the type of failure time distribution has a significant effect on the resilience; and (ii) the resilience increases with decreasing number of VNFs, while the availability increases with increasing number of UMEC hosts and the reliability decreases with increasing number of UMEC hosts, which can provide meaningful guidance for the UAV placement optimization in the UMEC network.**

***Keywords*—Resilience, Resource Degradation, Semi-Markov Process, Unmanned Aerial Vehicle**

I. Introduction

Network function virtualization (NFV) and multi-access edge computing (MEC) [1] technologies are opening up new opportunities to realize the vision of the fifth generation of mobile communications (5G) [2]. MEC brings storage and computation capacities to the edge of the network, allowing data processing, analysis, and transmission closer to the user side [3]. NFV can decouple network functions from expensive and dedicated hardware [4], thus providing network services by chaining virtualized network functions (VNFs) as service function chains (SFCs) [5]. The integration of NFV and MEC technologies plays a key role in provision of 5G services with strict performance requirements [6]. Nevertheless, factors such as mobility, high user density, and variations in radio coverage can pose a challenge for 5G to provide consistent network performance in both urban and rural settings. Unmanned aerial vehicle (UAV)-based MEC (UMEC), where UAVs serve as computing nodes to improve a potential of MEC networks, is emerging as a promising technology to provide ubiquitous computing supports and reliable communication to end users while avoiding costly investments in fixed infrastructure [7][8]. It has great potential for civilian and military applications, including but not limited to disaster recovery and response, traffic accident management, collision avoidance, and polar weather monitoring, among others [9]. In addition, the bursty resource requirements in vehicular network can be met by flexible and removable MEC servers deployed in mobile compute nodes (namely, UAVs) [10].

In the UMEC network, UMEC server is deployed on a UAV [11] and VNF is implemented as a lightweight container running on UMEC host operating system (OS) due to the limited resources and capabilities of UAV [12]. However, UMEC network with a large attack surface makes the system more vulnerable to attack, such as Denial-of-Service (DoS) attack [13]. Furthermore, the existence of container environments also provides a favorable condition for attackers. In the UMEC system, VNFs and host OSes can be subject to DoS attacks, resulting in resource degradation and even disruption of UMEC services [14]. Resource degradation can reduce the resilience of UMEC services and further lead to user QoS (Quality of Service) degradation.

Rejuvenation techniques, such as the failover technique and the live container migration technique, can mitigate the effects of resource degradation [15]. Once network service providers commit to a service level agreement (SLA) with the user, the resilience assessment is required to monitor SLA compliance and avoid being penalized for SLA violations [16]. Thus, it is necessary to evaluate the effectiveness of rejuvenation techniques from the aspects of availability and reliability and then to improve the resilience of UMEC services.

Analytical modeling is a kind of effective assessment approaches [17]. Various studies have been conducted on UMEC networks, but they focused on resource management and UAV placement optimization. There is little research on the resilience evaluation of the UMEC service chain consisting of multiple VNFs based on the analytical modeling approach. There were several analytical models to investigate the availability and/or reliability in a virtualized system. They often assumed that all time intervals between events were

- Jing Bai and Xiaolin Chang are with Beijing Key Laboratory of Security and Privacy in Intelligent Transportation, Beijing Jiaotong University, China. E-mail: {19112047, xlchang}@ bjtu.edu.cn. Xiaolin Chang is the corresponding author.
- Ricardo J. Rodríguez is with Departamento de Informática e Ingeniería de sistemas, Universidad de Zaragoza, Zaragoza, Spain. E-mail: rjrodriguez@unizar.es.
- Kishor S. Trivedi is with Department of Electrical and Computer Engineering, Duke University. E-mail: ktrivedi@duke.edu.
- Shupan Li is with School of Information Engineering, Zhengzhou University, Zhengzhou, China. E-mail: iespli@zzu.edu.cn.

exponentially distributed [26]-[28] and ignored time-dependent behaviors between VNFs and host OSes [26]-[32]. In addition, many studies only evaluated one of transient availability, steady-state availability and reliability [27]-[30]. Therefore, there are still some issues to be solved when assessing the resilience of UMEC service chains. In particular:

- UMEC service chain can consist of multiple VNFs. Each VNF can run on a separate UMEC host or co-exists with more than one VNF. Therefore, considering the relationship between the number of VNFs and UMEC hosts, how to quantitatively analyze the resilience of the UMEC service chain consisting of any number of VNFs executed in any number of UMEC hosts is an issue that needs to be addressed.
- There are time dependencies between the abnormal and recovery behaviors of VNFs and host OSes in UMEC system. For example, if a host OS fails, all VNFs running on this host OS are unavailable, while other VNFs not running on this host OS will not be affected. Therefore, how to capture time-dependent behavior between VNFs and host OSes is an issue that needs to be addressed.
- In a real UMEC system, the time intervals between some events follow non-exponential distributions. For example, the failure rates of VNFs and host OSes affected by resource degradation increase over time. Therefore, how to make the time intervals between events follow any kind of distribution to describe the behaviors of the system more precisely is an issue that needs to be addressed.

These discussions motivate the work presented in this paper. We propose a quantitative modeling approach to model the behaviors of a UMEC system that deploys multiple rejuvenation techniques for the recovery of VNFs and Host OSes experiencing resource degradation and failure. To the best of our knowledge, it is the first time that the resilience of UMEC service chains consisting of multiple VNFs has been quantitatively investigated on the condition that recovery time and failure time follow any kind of distribution. The main contributions are summarized as follows:

- We propose a multi-dimensional semi-Markov process (SMP) model to capture the recovery and abnormal (failure and resource degradation) behaviors of a UMEC system with any number of VNFs executed in any number of Primary UMEC Hosts. Specifically, our model can represent the time-dependent behaviors between VNFs and Host OSes that run them, between VNFs, and between Host OSes.
- We derive the formulas to calculate the transient availability, steady-state availability and reliability of a UMEC service chain consisting of n VNFs executed in m Primary UMEC Hosts ($m \le n$).
- We verify the approximate accuracy of our model and formulas by comparing the simulation results and the numerical results and carry out extensive numerical experiments. The sensitivity analysis indicates that migration time is the parameter significantly affecting the resilience. The numerical experiments investigating the impact of the number of VNFs and Primary UMEC Hosts and failure time distribution on the resilience illustrate that: (i) the type of failure time distribution has a significant effect on the resilience; and (ii) the availability of a UMEC service chain decreases with decreasing number of Primary UMEC Hosts, while its reliability increases with decreasing number of Primary UMEC Hosts.

The rest of this paper is organized as follows. Section II presents the background on the UMEC system and the related work on UMEC networks and resilience evaluation. Section III details the SMP model for the UMEC system. Section IV introduces the results of experiments. Section V discusses the limitation with our work and the possible solution. Section VI concludes the paper and states future work.

II. Related Work

This section first introduces the background on the UMEC system. Secondly, we presents the existing studies of UMEC networks. Finally, we introduce the existing studies of analytical modeling in the virtualized system, which are closely related to our work.

A. Background

Researches are taking the first steps towards realizing the NFV over mobile ad-hoc networks built by UAVs. OSM (Open Source MANO) PoC 10 demonstrated the practical feasibility of the VNF deployment over UAVs, where OSM is an ETSI (European Telecommunications Standards Institute)-hosted project [18]. In the UMEC system, multiple VNFs combined into one UMEC service chain are implemented with different containers running on multiple Primary UMEC Host OSes. All VNFs within the UMEC service chain are processed sequentially. Thus, the UMEC system mainly consists of a ground control station (GCS), multiple Primary UMEC Hosts, and Backup UMEC Hosts. The Primary UMEC Host OS runs one or more active containers and multiple backup containers to support the failover technique. The corresponding Backup UMEC Host is used to support the live container migration technique. Fig. 1 shows an example of UMEC system architecture, in which a UMEC service chain consists of four VNFs executed in three Primary UMEC Hosts. VNF and Host OS can experience resource degradation and failures caused by resource degradation. Resource degradation and failure behaviors of each VNF and Host OS are independent. However, there is a dependency between VNF and Host OS that runs it. That is, if the Host OS fails due to resource degradation, the VNF running on it will fail as well. Once resource degradation and failure events occur, the GCS immediately detects them correctly. Specific situations are as follows.

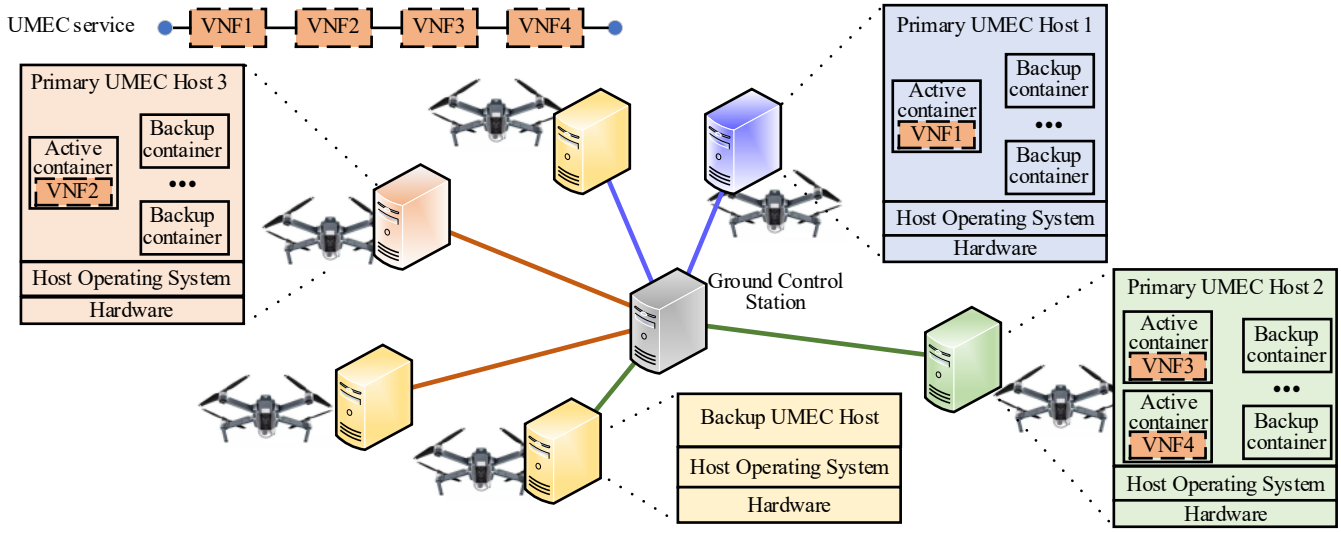

Fig. 1. A UMEC system architecture with four VNFs and three Primary UMEC Hosts

TABLE I
Comparisons of Existing Models

No.	System		Resource Degradation Behavior	Multiple Interaction	State-space Model	Solution Type		Distribution		Metric		Simulation
	Hypervisor-based	*Container-based*				*Steady-state*	*Transient*	*Exponential*	*General*	*Availability*	*Reliability*	
[24][25]	√	×	×	×	×	√	×	×	×	×	√	√
[26]	√	×	√	×	√	√	√	√	×	√	√	×
[27]	√	×	×	×	√	√	×	√	×	√	×	√
[28]	×	√	×	×	√	√	×	√	×	√	×	×
[29]	√	×	×	×	√	√	×	√	√	√	×	×
[30]	√	×	√	×	√	√	×	√	√	√	×	×
[31]	×	√	√	×	√	√	√	√	√	√	√	√
[32]	×	×	√	×	√	√	√	√	√	√	√	√
Ours	×	√	√	√	√	√	√	√	√	√	√	√

a. 'System' column indicates whether system considered in the corresponding paper is a hypervisor-based or container-based system.
b. 'Resource' column indicates whether the resource degradation behaviors of components are considered in the corresponding paper.
c. 'Multiple Interaction' column indicates whether the time-dependent behaviors between VNFs, between Host OSes and between VNFs and Host OSes are considered in the corresponding paper.
d. 'State-space' column indicates whether the state-space model is conducted in the corresponding paper.
e. 'Solution Type' indicates whether transient analysis or steady-state analysis is performed in the corresponding paper.
f. 'Distribution' column indicates whether exponential distribution or general distribution is assumed in the corresponding paper.
g. 'Metric' column indicates whether the transient availability, steady-state availability or reliability is evaluated in the corresponding paper.
h. 'Simulation' column indicates whether simulation is carried out in the corresponding paper.

If the GCS detects resource degradation on an active VNF, the failover technique is triggered and the backup container will take over the processing requests. Then the container running the VNF with resource degradation is restarted to its initial state. After this container completes its restarting, it becomes the backup container for the next failover.

If the GCS detects resource degradation on a Primary UMEC Host OS, the live container migration technique is triggered and the Backup UMEC Host OS will take over the processing requests. The degraded Host OS then reboots to its initial state. After this Host OS completes its reboot, this host becomes the Backup UMEC Host for the next container migration.

If multiple VNFs (more than one) running on the same Host OS or an active VNF and Host OS running it experience resource degradation, this Host OS reboots. If multiple Primary UMEC Host OSes (more than one) or an active VNF and Primary UMEC Host OSes running other active VNFs experience resource degradation, all Host OSes in the UMEC system are rebooted. If multiple active VNFs (more than one) running on different Primary UMEC Host OSes experience resource degradation, all active VNFs in the UMEC system are restarted.

If any active VNF or Primary UMEC Host OS in the UMEC system fails due to resource degradation, the service is interrupted because all active VNFs within the UMEC service chain are processed sequentially and the dependencies among VNF, container and Host OS. After the Host OS repair is complete, the Host OSes, containers, VNFs and requests are rebooted/restarted in sequence.

B. UAV-based MEC Network

In the last few years, many studies have been devoted to optimizing UAV placement and managing resources in the UMEC network. Li *et al.* [19] presented an optimization approach to minimize the energy consumption of a UMEC

system, considering the resource allocation and the design of the UAV trajectory. Zhang *et al*. [20] studied an iterative optimization algorithm to optimize user association, computing and communication resource allocation, and UAV trajectory scheduling in a UMEC system. Zhang *et al*. [21] proposed a game-theoretic scheme to achieve the trade-off between energy consumption and time latency. Kang *et al*. [22] jointly optimized task scheduling and UAV trajectory to minimize the maximum task processing delay. Furthermore, there were many studies to evaluate the resilience of a UAV swarm. Bai *et al*. [23] presented a UAV swarm model that considered the impact of distance between UAVs and dynamic change, and an resilience metric that reflected the difference between the performance of UAV swarm and the performance of standard system. However, the authors in [23] only considered the failure caused by external disruptions and threats. In this paper, the UMEC system can suffer from resource degradation and failure. Note that our work can complement these studies to better study the mission planning and the design of a UAV swarm.

C. Analytical Modeling

Researches have explored analytical modeling approaches to evaluate the availability and reliability in the virtualized system. See [24]-[32] and references therein.

Qu *et al*. [24] investigated the reliability of SFC under the strategy that used different backup VNFs to protect the primary VNF based on reliability block diagrams (RBD). Engelmann *et al*. [25] analyzed the reliability of SFC under different placement strategies for primary and backup VNFs based on RBD. These studies [24][25] assumed that abnormal and recovery behaviors of VNFs were independent of each other and did not capture the dynamic interaction between various behaviors. Torquato *et al*. [26] built stochastic reward net (SRN) models for evaluating the reliability and availability of a virtualization system, in which virtual machine (VM) migration technique was deployed for rejuvenation. Tola *et al*. [27] combined structural model and stochastic activity network (SAN) model to evaluate the impact of network factors on NFV-enabled service availability. Mauro *et al*. [28] studied the availability of IP Multimedia Subsystem in different containerized architectural deployments based on SRN. These studies [26]-[28] assumed that all time intervals between events were exponentially distributed. In this paper, we relax this assumption and allow recovery time and failure time to follow any kind of distribution. There were modeling-based studies [29]-[32] in which all time intervals between events followed any kind of distribution. Machida *et al*. [29] proposed SMP models to compare the effectiveness of time-based rejuvenation, time-based life-extension and hybrid approaches, from the aspects of job completion time and system availability. Based on Markov regenerative process (MRGP), the authors in [30] studied the service availability in the VM-based system, in which application service, VM and virtual machine monitor (VMM) can experience resource degradation. They in [31] presented an SMP model to analyze the vehicle platooning service resilience. They further in [32] analyzed the impact of VNF aging on the dependability on MEC-SFC services. These model in [30]-[32] did not capture the time-dependent behaviors between the subservices and the Host OSes that run them. These studies [24]-[32] ignored time-dependent behaviors between VNFs, between Host OSes, and between VNFs and Host OSes. In addition, some studies [24][25][27]-[30] evaluated only one or two aspects of reliability, steady-state availability and transient availability. Unlike them, we consider a two-tier (VNF and Host OS) UMEC system, in which VNF restart and failover techniques are deployed for rejuvenation at the VNF level, and OS reboot and live container migration are deployed for rejuvenation at the Host OS level. We present an SMP model to characterize the interactions between components and evaluate the reliability, steady-state availability and transient availability of a UMEC service chain consisting of any number of VNFs executed in any number of Primary UMEC Hosts.

TABLE I summarizes the comparison of existing work on evaluating the resilience using analytical modeling approaches.

III. System Model

This section first introduces the multi-dimensional SMP model proposed in this paper. Secondly, formulas are given to calculate MTTF (the mean time to failure), steady-state availability and transient availability of the *n*-sized UMEC service chain.

A. SMP Model

The system state transition can be described by a stochastic process $\{Z(t)|t \geq 0\}$. The sequence of system states $X = \{X_0, X_1, X_2, X_3, X_4, X_5, ...\}$ (including the occurrence of resource degradation events, failure events, and recovery events) corresponding to time instances $T = \{T_0, T_1, T_2, T_3, T_4, T_5, ...\}$, in which this stochastic process undergoes state transitions, is the embedded discrete time Markov chain (DTMC). We assume that the holding times of the recovery and failure events follow any kind of distribution and the holding times of resource degradation events are exponentially distributed. Thus, SMP model can be used to capture the recovery and abnormal behaviors of the n-sized UMEC system, where the number of backup containers must be greater than that of active containers in Primary UMEC Host. In this model, failover, live container migration, VNF restart and OS reboot will bring the container-based UMEC system to an error-free state. The timer to be used for next the failover, container migration, VNF restart or OS reboot is restarted after completing failover, container migration, VNF restart, or OS reboot.

We define the (n+m)-tuple index $(i_1, i_2, ..., i_u, ..., i_m, j_{11}, j_{12}, ..., j_{1n_1}, ..., j_{m1}, j_{m2}, ..., j_{mw}, ..., j_{mn_m})$ to denote the system state. n and m denote the number of VNFs and OSes, respectively. That is, a UMEC service chain consists of n VNFs hosted by m Primary UMEC Hosts. nm denotes the number of VNFs hosted by the mth Primary UMEC Host OS. Thus, $n_1 + n_2 + ,..... , + n_m = n$ and $m \leq n$. i_m, j_{mw}, j_{mn_m} denote the state of the mth Primary UMEC Host OS, the wth VNF running on the mth Primary UMEC Host OS and the nmth VNF running

on the mth Primary UMEC Host OS, respectively. There are four VNF (Host OS) states: Healthy, Failed, Resource Degradation and Restart/Reboot, denoted by H, F, D and R, respectively. The meaning of each VNF (Host OS) state is given as follows:

- Healthy. The VNF (Host OS) is robust and UMEC service chain can be performed normally. Rejuvenation techniques can return the VNF (Host OS) experiencing resource degradation to this state.
- Failed. The UMEC service chain is unavailable due to VNF (Host OS) failure at this state.
- Resource Degradation. The VNF (Host OS) can function but experiences resource degradation at this state.
- Restart/Reboot. At this state, the VNF (Host OS) restarts (reboots).

There are a total of 4^{m+n} system states, among which there are $4^{m+n}-2m-n-4$ meaningless system states. These meaningless states can be ignored. Take system state $(F_1, H_2, ..., H_m, H_{11}, H_{12}, ..., H_{1n_1}, ..., H_{mn_m})$ for example, if the 1st Primary UMEC Host OSes fails, the VNFs running on this OS will fail due to the dependencies between VNF and OS. Therefore, this system state is meaningless. TABLE II gives the definition of the time intervals between events, where $d_{UU}(t)=\sqrt{(x_u(t)-x_{bu}(t))^2+(y_u(t)-y_{bu}(t))^2+(z_u(t)-z_{bu}(t))^2}$ and $d_{US}(t)=\sqrt{(x_u(t)-x_s(t))^2+(y_u(t)-y_s(t))^2+(z_u(t)-z_s(t))^2}$ denote the distance between the UAV deploying the uth Primary UMEC Host OS and the UAV deploying the uth Backup UMEC Host OS, and the distance between the UAV deploying the uth Primary UMEC Host OS and user s, respectively. Note that the position $(x_u(t), y_u(t), z_u(t))$ ($(x_{bu}(t), y_{bu}(t), z_{bu}(t))$) of UAV u and the position $(x_s(t), y_s(t), z_s(t))$ of user s can vary over time. According to UAV-UAV and UAV-user channel models [33][34], the distances between UAVs and between UAV and its serving user have an impact on the data transmission rates between them, which may further affect the resource degradation time, failure time and migration time defined in TABLE II.

For case of understanding, Fig. 2 shows an example of the SMP model for capturing the behaviors of a 4-sized UMEC system with three Primary UMEC Host OSes running one, one and two VNFs, respectively. In Fig. 2, the green system state denotes that the requests can be processed normally, the yellow system states denote that one of system components experiences resource degradation, the grey system states denote that some system components are recovering, the purple system state denotes a failure state, the black straight lines denote the resource degradation behaviors of components, the orange dash-dotted lines denote the failure behaviors of components, and the blue dashed lines denote the recovery behaviors of components. TABLE II shows the definition of variables used in the model. In this model, the UMEC system starts with state 0. After a period of operation, the components in the system can experience resource degradation and the system enters one of the yellow states in Fig. 2 depending on the component that experiences resource degradation. When the system stays at state 10, if the backup container takes over the processing requests, the system will enter state 0, if the 1st VNF fails, the system will enter state 1, if one of the 2nd and 3rd Primary UMEC Host OSes experiences resource degradation, the system will enter state 2, if one of the remaining VNFs experiences resource degradation, the system will enter state 3, and if the 1st Primary UMEC Host OS experiences resource degradation, the system will enter state 4. When the system stays at state 3, the system either enters state 0 after restarting all VNFs, or enters state 2 after one of the Primary UMEC Host OSes experiences resource degradation. When the system stays at state 4, the system either enters state 0 after rebooting the 1st Primary UMEC Host OS or enters state 2 after one of the 2nd Primary UMEC Host OS, the 3rd Primary UMEC Host OS and VNFs running on them experiences resource degradation. From state 1, the system returns back to state 0 after repairing the failed component and rebooting all Host OSes. From state 2, the system returns back to state 0 after rebooting all OSes. The subsequent state transitions of the system at state 7, 8, 9, 11, 12 and 13 are similar to that of the system at state 10.

B. Transient Availability Analysis

We present the calculation process of the transient availability in this section.

Firstly, the kernel matrix $\mathbf{K}_{UM}(t)$ is constructed, given in Fig. 3. The non-null element $k_{ij}(t)$ ($0 \le i \le 2m+n+3$, $0 \le j \le 2m+n+3$) in $\mathbf{K}_{UM}(t)$ denotes the conditional probability of the next transition to system state j occurring at time t, given that at time T_n, the UMEC system has stayed at state i. The formulas of calculating the non-mull elements of $\mathbf{K}_{UM}(t)$ are given in Equations (A.1)-(A.17) in Appendix A of the supplementary file. Secondly, we can get the diagonal matrix $\mathbf{E}_{UM}(t)=[E_{ii}(t)]$ ($0 \le i \le 2m+n+3$), which can be solved by applying Equation (1).

$$E_{ii}(t)=1-\sum_{j=0}^{2m+n+3} k_{ij}(t) \tag{1}$$

Thirdly, the matrix $\mathbf{V}_{UM}(t)=[V_{ij}(t)]$ ($0 \le i \le 2m+n+3$, $0 \le j \le 2m+n+3$) of the transient solution for the conditional transition probability can be solved by applying Equation (2) [17],

$$\tilde{\mathbf{V}}_{UM}(s)=\tilde{\mathbf{E}}_{UM}(s)+\tilde{\mathbf{K}}_{UM}(s)\tilde{\mathbf{V}}_{UM}(s) \tag{2}$$

where $\tilde{\mathbf{V}}_{UM}(s)$, $\tilde{\mathbf{E}}_{UM}(s)$ and $\tilde{\mathbf{K}}_{UM}(s)$ are Laplace-Stieltjes transform of $\mathbf{V}_{UM}(t)$, $\mathbf{E}_{UM}(t)$ and $\mathbf{K}_{UM}(t)$, respectively.

Finally, we can obtain the unconditional probabilities $\pi_{UM}(t)=[\pi_i(t)]$ by using Equation (3) [17],

$$\pi_{UM}(t)=\pi_{UM}(0)\mathbf{V}_{UM}(t) \tag{3}$$

where $\pi_{UM}(0)$ is the initial state probability vector. The initial state probability at system state 0 is 1 and the initial state probabilities at the remaining system states are 0. The transient availability of *n*-sized UMEC service chain is computed by applying Equation (4).

$$\mathrm{A}_{TUM}(t) = 1 - \sum_{i=1}^{m+3} \pi_i(t) \tag{4}$$

The detailed process for calculating $\pi_i(t)$ is given in Equations (A.18)-(A.21) in Appendix A of the supplementary file.

C. Steady-state Availability Analysis

We present the calculation process of the steady-state availability.

Firstly, in order to describe the embedded DTMC in the SMP model, we construct the one-step transition probability matrix (TPM) $\mathbf{P}_{UM} = \lim_{t\to\infty} \mathbf{K}_{UM}(t)$. Secondly, we use Equation (5) to obtain the steady-state probability vector $\mathbf{V}_{UM}^{*} = [V_i^{*}]$ of the embedded DTMC in the SMP model [17],

$$\mathbf{V}_{UM}^{*} = \mathbf{V}_{UM}^{*}\mathbf{P} \text{ subject to } \mathbf{V}_{UM}^{*} e^{\mathrm{T}} = 1 \tag{5}$$

where e denotes a column vector with all items are 1. The formulas for calculating elements in $\mathbf{V}_{UM}^{*}$ are given in Equations (B.1)-(B.6) in Appendix B of the supplementary file. Thirdly, the mean sojourn time h_i^{*} at system state i is calculated by using Equation (6) [17],

$$h_i^{*} = \int_0^{\infty} (1 - G_i(t))dt \tag{6}$$

where $G_i(t)$ denotes the sojourn time distribution at system state i. The detailed process for calculating the mean sojourn times at each system state is given in Equations (B.7)-(B.13) in Appendix B of the supplementary file.

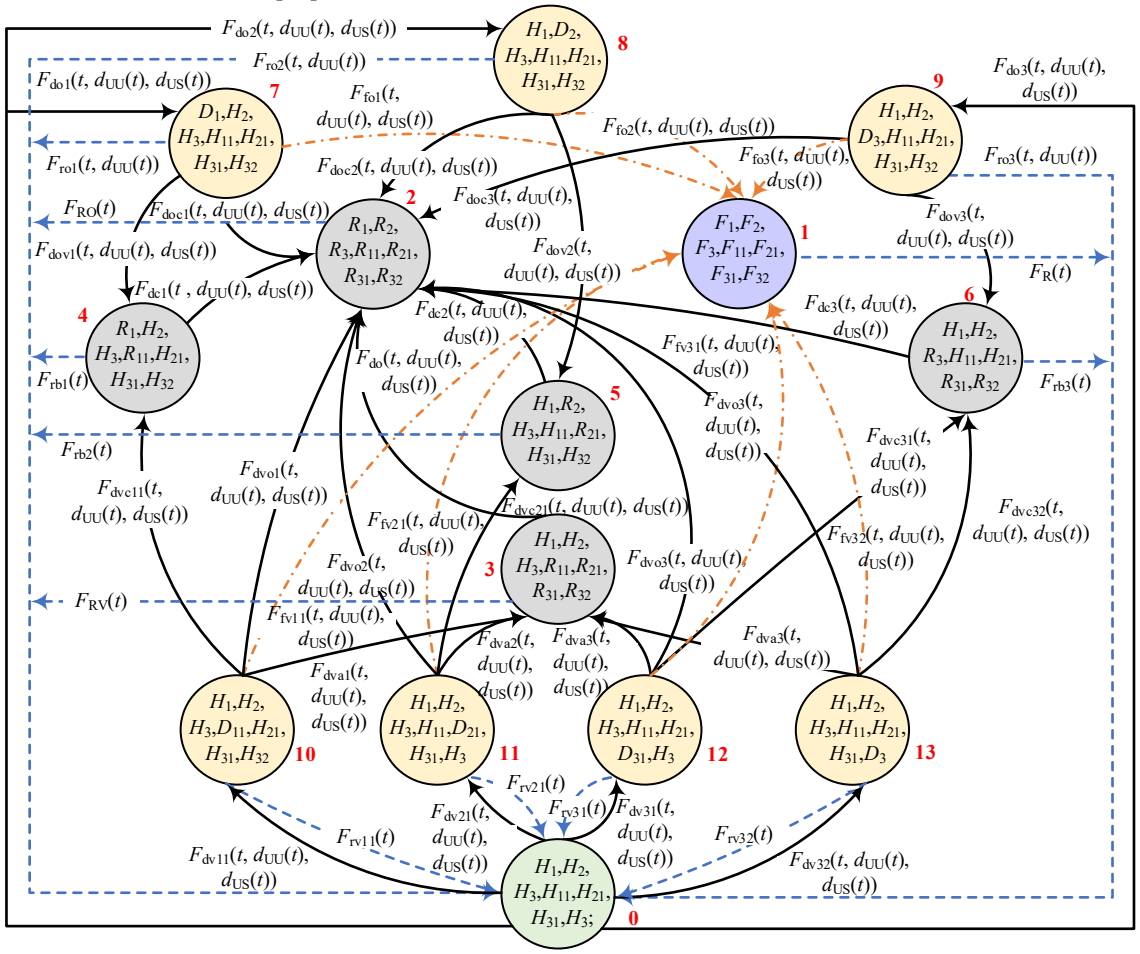

Fig. 2. SMP model for a UMEC system with four VNFs and three Primary UMEC Hosts

$$\mathbf{K}_{UM}(t) = \begin{pmatrix}
0 & 0 & 0 & 0 & 0 & \cdots & 0 & k_{0(m+4)}(t) & \cdots & k_{0(2m+4)}(t) & \cdots & k_{0(2m+3+n)}(t) \\
k_{10}(t) & 0 & 0 & 0 & 0 & \cdots & 0 & 0 & \cdots & 0 & \cdots & 0 \\
k_{20}(t) & 0 & 0 & 0 & 0 & \cdots & 0 & 0 & \cdots & 0 & \cdots & 0 \\
k_{30}(t) & 0 & k_{32}(t) & 0 & 0 & \cdots & 0 & 0 & \cdots & 0 & \cdots & 0 \\
k_{40}(t) & 0 & k_{42}(t) & 0 & 0 & \cdots & 0 & 0 & \cdots & 0 & \cdots & 0 \\
\cdots & \cdots & \cdots & \cdots & \cdots & \ddots & \cdots & \cdots & \ddots & \cdots & \ddots & \cdots \\
k_{(m+3)0}(t) & 0 & k_{(m+3)2}(t) & 0 & 0 & \cdots & 0 & 0 & \cdots & 0 & \cdots & 0 \\
k_{(m+4)0}(t) & k_{(m+4)1}(t) & k_{(m+4)2}(t) & 0 & k_{(m+4)4}(t) & \cdots & 0 & 0 & \cdots & 0 & \cdots & 0 \\
\cdots & \cdots & \cdots & \cdots & \cdots & \ddots & \cdots & \cdots & \ddots & \cdots & \ddots & \cdots \\
k_{(2m+4)0}(t) & k_{(2m+4)1}(t) & k_{(2m+4)2}(t) & k_{(2m+4)3}(t) & k_{(2m+4)4}(t) & \cdots & 0 & 0 & \cdots & 0 & \cdots & 0 \\
\cdots & \cdots & \cdots & \cdots & \cdots & \ddots & \cdots & \cdots & \ddots & \cdots & \ddots & \cdots \\
k_{(2m+3+n)0}(t) & k_{(2m+3+n)1}(t) & k_{(2m+3+n)2}(t) & k_{(2m+3+n)3}(t) & 0 & \cdots & k_{(2m+3+n)(m+3)}(t) & 0 & \cdots & 0 & \cdots & 0
\end{pmatrix}$$

Fig. 3. The kernel matrix $\mathbf{K}_{UM}(t)$

TABLE II
Definition of Variables Used in the Model

Symbol	Definition	Distribution	Type	Default Values
$T_{\mathrm{dv}ij}$	A random variable with cumulative distribution function (CDF) $F_{\mathrm{dv}ij}(t, d_{\mathrm{UU}}(t), d_{\mathrm{US}}(t))$ denoting the holding time of the j^{th} active VNF running on the i^{th} Primary UMEC Host OS from H to D.	Exponential	Resource degradation time	9-11 days
$T_{\mathrm{do}i}$	A random variable with CDF $F_{\mathrm{do}i}(t, d_{\mathrm{UU}}(t), d_{\mathrm{US}}(t))$ denoting the holding time of the i^{th} of Primary UMEC Host OS from H to D.	Exponential	Resource degradation time	45-47 days
$T_{\mathrm{fv}ij}$	A random variable with CDF $F_{\mathrm{fv}ij}(t, d_{\mathrm{UU}}(t), d_{\mathrm{US}}(t))$ denoting the holding time of the j^{th} active VNF (running on the i^{th} Primary UMEC Host OS) from D to F.	General	Failure time	6-8 days
$T_{\mathrm{fo}i}$	A random variable with CDF $F_{\mathrm{fo}i}(t, d_{\mathrm{UU}}(t), d_{\mathrm{US}}(t))$ denoting the holding time of the i^{th} Primary UMEC Host OS from D to F.	General	Failure time	15-17 days
$T_{\mathrm{rv}ij}$	A random variable with CDF $F_{\mathrm{rv}ij}(t)$ denoting the holding time of the j^{th} active VNF (running on the i^{th} Primary UMEC Host OS) from D to H.	General	Failover time	8-10 seconds
$T_{\mathrm{ro}i}$	A random variable with CDF $F_{\mathrm{ro}i}(t, d_{\mathrm{UU}}(t))$ denoting the holding time of the i^{th} Primary UMEC Host OS from D to H.	General	Migration time	30-40 seconds
$T_{\mathrm{rb}i}$	A random variable with CDF $F_{\mathrm{rb}i}(t)$ denoting the holding time of rebooting the i^{th} Primary UMEC Host OS.	General	Reboot time	1-1.5 minutes
T_{RV}	A random variable with CDF $F_{\mathrm{RV}}(t)$ denoting the holding time to restart all VNFs.	General	Restart time	10-20 seconds
T_{RO}	A random variable with CDF $F_{\mathrm{RO}}(t)$denoting the holding time to reboot all Host OSes.	General	Reboot time	1-2 minutes
T_{R}	A random variable with CDF $F_{\mathrm{R}}(t)$ denoting the holding time of the system from failure to robustness.	General	System repair time	0.8-1.2 hours
$T_{\mathrm{dvo}i}$	A random variable with CDF $F_{\mathrm{dvo}i}(t, d_{\mathrm{UU}}(t), d_{\mathrm{US}}(t))$ denoting the minimum holding time of Primary UMEC Host OSes (in addition to the i^{th} Primary UMEC Host OS) from H to D after the active VNF (running on the i^{th} Primary UMEC Host OS) experiencing resource degradation.	Exponential	Resource degradation time	--
$T_{\mathrm{dvc}ij}$	A random variable with CDF $F_{\mathrm{dvc}ij}(t, d_{\mathrm{UU}}(t), d_{\mathrm{US}}(t))$ denoting the minimum holding time of other active VNFs (running on the i^{th} Primary UMEC Host OS) and i^{th} Primary UMEC Host OS from H to D after the j^{th} active VNF (running on the i^{th} Primary UMEC Host OS) experiencing resource degradation.	Exponential	Resource degradation time	--
$T_{\mathrm{dva}i}$	A random variable with CDF $F_{\mathrm{dva}i}(t, d_{\mathrm{UU}}(t), d_{\mathrm{US}}(t))$ denoting the minimum holding time of other active VNFs (in addition to the active VNFs running on the i^{th} Primary UMEC Host OS) from H to D after the j^{th} active VNF (running on the i^{th} Primary UMEC Host OS) experiencing resource degradation.	Exponential	Resource degradation time	--
$T_{\mathrm{doc}i}$	A random variable with CDF $F_{\mathrm{doc}i}(t, d_{\mathrm{UU}}(t), d_{\mathrm{US}}(t))$ denoting the minimum holding time of other components (in addition to the active VNFs running on the i^{th} Primary UMEC Host OS) from H to D after the i^{th} Primary UMEC Host OS experiencing resource degradation.	Exponential	Resource degradation time	--
$T_{\mathrm{dov}i}$	A random variable with CDF $F_{\mathrm{dov}i}(t, d_{\mathrm{UU}}(t), d_{\mathrm{US}}(t))$ denoting the minimum holding time of the active VNFs (running on the i^{th} Primary UMEC Host OS) from H to D after this Host OS experiencing resource degradation.	Exponential	Resource degradation time	--
$T_{\mathrm{dc}i}$	A random variable with CDF $F_{\mathrm{dc}i}(t, d_{\mathrm{UU}}(t), d_{\mathrm{US}}(t))$ denoting the minimum holding time of other components from H to D after both the active VNF (running on the i^{th} Host OS) and this Host OS experiencing resource degradation.	Exponential	Resource degradation time	--
T_{do}	A random variable with CDF $F_{\mathrm{do}}(t, d_{\mathrm{UU}}(t), d_{\mathrm{US}}(t))$ denoting the minimum holding time of each Primary UMEC Host OS from H to D during restarting all VNFs.	Exponential	Resource degradation time	--

$$\mathbf{K}'_{UM}(t)=\begin{pmatrix} 0 & k'_{01}(t) & \cdots & k'_{0(m+1)}(t) & \cdots & k'_{0(m+n)}(t) & 0 & \cdots & 0 & 0 & 0 & 0 \\ k'_{10}(t) & 0 & \cdots & 0 & \cdots & 0 & k'_{1(m+n+1)}(t) & \cdots & 0 & k'_{1(2m+n+1)}(t) & k'_{1(2m+n+2)}(t) & 0 \\ \cdots & \cdots & \ddots & \cdots & \ddots & \cdots & \cdots & \ddots & \cdots & \cdots & \cdots & \cdots \\ k'_{(m+1)0}(t) & 0 & \cdots & 0 & \cdots & 0 & k'_{(m+1)(m+n+1)}(t) & \cdots & 0 & k'_{(m+1)(2m+n+1)}(t) & k'_{(m+1)(2m+n+2)}(t) & k'_{(m+1)(2m+n+3)}(t) \\ \cdots & \cdots & \ddots & \cdots & \ddots & \cdots & \cdots & \ddots & \cdots & \cdots & \cdots & \cdots \\ k'_{(m+n)0}(t) & 0 & \cdots & 0 & \cdots & 0 & 0 & \cdots & k'_{(m+n)(2m+n)}(t) & k'_{(m+n)(2m+n+1)}(t) & k'_{(m+n)(2m+n+2)}(t) & k'_{(m+n)(2m+n+3)}(t) \\ 0 & 0 & \cdots & 0 & \cdots & 0 & 1 & \cdots & 0 & 0 & 0 & 0 \\ \cdots & \cdots & \ddots & \cdots & \ddots & \cdots & \cdots & \ddots & \cdots & \cdots & \cdots & \cdots \\ 0 & 0 & \cdots & 0 & \cdots & 0 & 0 & \cdots & 1 & 0 & 0 & 0 \\ 0 & 0 & \cdots & 0 & \cdots & 0 & 0 & \cdots & 0 & 1 & 0 & 0 \\ 0 & 0 & \cdots & 0 & \cdots & 0 & 0 & \cdots & 0 & 0 & 1 & 0 \\ 0 & 0 & \cdots & 0 & \cdots & 0 & 0 & \cdots & 0 & 0 & 0 & 1 \end{pmatrix}$$

Fig. 4. The kernel matrix $\mathbf{K}'_{UM}(t)$ for the SMP model with absorbing states

The steady-state availability of n-sized UMEC service chain is computed by applying Equation (7).

$$\mathrm{A}_{SUM}=1-\left(\sum_{j=1}^{m+3}V_j^*h_j^*\right)\Bigg/\left(\sum_{i=0}^{2m+n+3}V_i^*h_i^*\right) \tag{7}$$

where V_j^*, h_j^*, V_i^* and h_i^* can be obtained by applying Equations (B.1)-(B.13) in Appendix B of the supplementary file.

D. Reliability Analysis

We present the calculation process of MTTF, which can be used to analyze the reliability of a UMEC service chain in this section.

MTTF is a classical yardstick for assessing the reliability. It is the expected time to failure for the UMEC system, in which no recovery operation is performed when the service failure occurs. Therefore, we can construct the SMP model with

absorbing states based on the SMP model proposed in Section III-*A*. That is, the grey and purple system states in Fig. 2 serve as the absorbing states.

Firstly, in order to obtain the one-step TPM $\mathbf{P}'_{UM}$ for describing the embedded DTMC in the SMP model with absorbing states, we construct the kernel matrix $\mathbf{K}'_{UM}(t)$ for this model, given in Fig. 4.The formulas of calculating non-null elements of $\mathbf{P}'_{UM}$ are given in Equations (C.1)-(C.16) in Appendix C of the supplementary file. We use Equation (8) to calculate the expected number of visits V'_i to system state i until absorption [17],

$$V'_i = \alpha_i + \sum_{j=0}^{m+n} V'_j p'_{ji} \tag{8}$$

where the initial probability α_0 at system state 0 is 1 and the initial probabilities α_i ($1 \le i \le m+n$) at the remaining system states are 0. The formulas of calculating the expected number of visits to each system state of this model are given in Equations (9) and (10),

$$V'_0 = -1 \Big/ \left(\sum_{i=1}^{m+n} p'_{0i} p'_{i0} - 1\right) \tag{9}$$

$$V'_i = -p'_{0i} \Big/ \left(\sum_{i=1}^{m+n} p'_{0i} p'_{i0} - 1\right) \tag{10}$$

where $1 \le i \le m+n$ and p'_{i0} and p'_{0i} can be obtained by applying Equations (C.1)-(C.3) and (C.7).

Thirdly, the mean sojourn times at each system state of the SMP with absorbing states are given in Equations (11)-(13),

$$h'_0 = \int_0^\infty \prod_{u=1}^{m} (1 - F_{\mathrm{do}u}(t, d_{UU}(t), d_{US}(t))) \prod_{u=1}^{m} \prod_{w=1}^{n_u} (1 - F_{\mathrm{dv}uw}(t, d_{UU}(t), d_{US}(t)))dt \tag{11}$$

$$h'_i = \int_0^\infty (1 - F_{\mathrm{fo}i}(t, d_{UU}(t), d_{US}(t)))(1 - F_{\mathrm{ro}i}(t, d_{UU}(t))) (1 - F_{\mathrm{dov}i}(t, d_{UU}(t), d_{US}(t)))(1 - F_{\mathrm{doc}i}(t, d_{UU}(t), d_{US}(t)))dt \tag{12}$$

$$h'_{(m+\sum_{q=0}^{i-1} n_q + j)} = \int_0^\infty (1 - F_{\mathrm{fv}ij}(t, d_{UU}(t), d_{US}(t)))(1 - F_{\mathrm{doc}i}(t, d_{UU}(t), d_{US}(t)))(1 - F_{\mathrm{rv}ij}(t))(1 - F_{\mathrm{dvc}ij}(t, d_{UU}(t), d_{US}(t))) (1 - F_{\mathrm{dva}i}(t, d_{UU}(t), d_{US}(t)))(1 - F_{\mathrm{dvo}i}(t, d_{UU}(t), d_{US}(t)))dt \tag{13}$$

where $1 \le i \le m$ and $1 \le j \le n_i$.

Finally, the MTTF of n-sized UMEC service chain is computed by applying Equation (14).

$$\mathrm{MTTF} = \sum_{i=0}^{m+n} V'_i h'_i \tag{14}$$

where V'_i and h'_i can be obtained by applying Equations (9)-(13).

IV. Experiment Results

This section, we first show the comparison of the numerical and simulation results to verify the approximate accuracy of the proposed model and formulas. We then perform the sensitivity analysis of MTTF, steady-state availability and transient availability of a UMEC service chain in regard to system parameters. Finally, we apply our proposed equations in Section III to quantitatively analyze the impact of system parameters (such as, the number of VNFs and Primary UMEC Hosts) and failure time distributions on each metric.

A. Experiment Configuration

In the numerical experiments, it is assumed that the VNF resource degradation time, OS resource degradation time, migration time, failover time, reboot time, restart time and system repair time are exponentially distributed. The corresponding distribution functions are $F_{\mathrm{do}i}(t, d_{UU}(t), d_{US}(t)) = EXP(\alpha_{oi})$, $F_{\mathrm{dv}ij}(t, d_{UU}(t), d_{US}(t)) = EXP(\alpha_{vij})$, $F_{\mathrm{ro}i}(t, d_{UU}(t), d_{US}(t)) = EXP(\gamma_{oi})$, $F_{\mathrm{rv}ij}(t) = EXP(\beta_{vij})$, $F_{\mathrm{rb}i}(t) = EXP(\delta_i)$, $F_{\mathrm{R}}(t) = EXP(\varepsilon)$, $F_{\mathrm{RO}}(t) = EXP(\varphi)$ and $F_{\mathrm{RV}}(t) = EXP(\mu)$, respectively, where $1 \le i \le m$ and $1 \le j \le n_i$. VNF failure time and OS failure time are assumed to follow Hypoexponential distributions, denoted as $F_{\mathrm{fo}i}(t, d_{UU}(t), d_{US}(t)) = HYPO(\lambda_{oi1}, \lambda_{oi2})$ and $F_{\mathrm{fv}ij}(t, d_{UU}(t), d_{US}(t)) = HYPO(\lambda_{vij1}, \lambda_{vij2})$ ($1 \le i \le m$ and $1 \le j \le n_i$), respectively. The holding times of other resource degradation events are assumed to be exponentially distributed, denoted as $F_{\mathrm{do}}(t, d_{UU}(t), d_{US}(t)) = EXP(\sum_{r=1}^{m} \alpha_{or})$, $F_{\mathrm{dvo}i}(t, d_{UU}(t), d_{US}(t)) = EXP(\sum_{u \in A_i} \alpha_{ou})$, $F_{\mathrm{dvc}ij}(t, d_{UU}(t), d_{US}(t)) = EXP(\alpha_{oi} + \sum_{v \in B_{ij}} \alpha_{viv})$, $F_{\mathrm{dva}i}(t, d_{UU}(t), d_{US}(t)) = EXP(\sum_{u \in A_i} \sum_{w=1}^{n_u} \alpha_{vuw})$, $F_{\mathrm{dov}i}(t, d_{UU}(t), d_{US}(t)) = EXP(\sum_{w=1}^{n_i} \alpha_{viw})$ and $F_{\mathrm{dc}i}(t, d_{UU}(t), d_{US}(t)) = F_{\mathrm{doc}i}(t, d_{UU}(t), d_{US}(t)) = EXP(\sum_{u \in A_i} \alpha_{ou} + \sum_{u \in A_i} \sum_{w=1}^{n_u} \alpha_{vuw})$, where $A_i = \{u | 1 \le u \le m, u \ne i\}$, $B_{ij} = \{v | 1 \le v \le n_i, v \ne j\}$, $1 \le i \le m$ and $1 \le j \le n_i$. The default parameter settings are given in TABLE II. Some parameters in experiments are set according to [35] and the left parameters are set in order to demonstrate the effectiveness of our model proposed in this paper. Numerical experiments and simulation are carried out in MAPLE [36].

B. Verification of the Proposed Model and Formulas

TABLE III shows the parameters used in the simulation. Fig. 3 (from left to right) shows the comparison of the numerical and simulation results for the transient availability, steady-state availability and MTTF. '*n*=15_*m*=5_num' denotes the numerical results on the condition that there are five Primary UMEC Hosts and fifteen VNFs in the UMEC system. The corresponding simulation results are denoted by '*n*=15_*m*=5_sim'. The simulation results of transient availability, steady-state availability and MTTF are calculated with a 95% confidence level. We observe that numerical results are close to the corresponding simulation results, demonstrating the approximate accuracy of the proposed model and formulas for calculating the transient availability, steady-state availability and MTTF of a UMEC service chain.

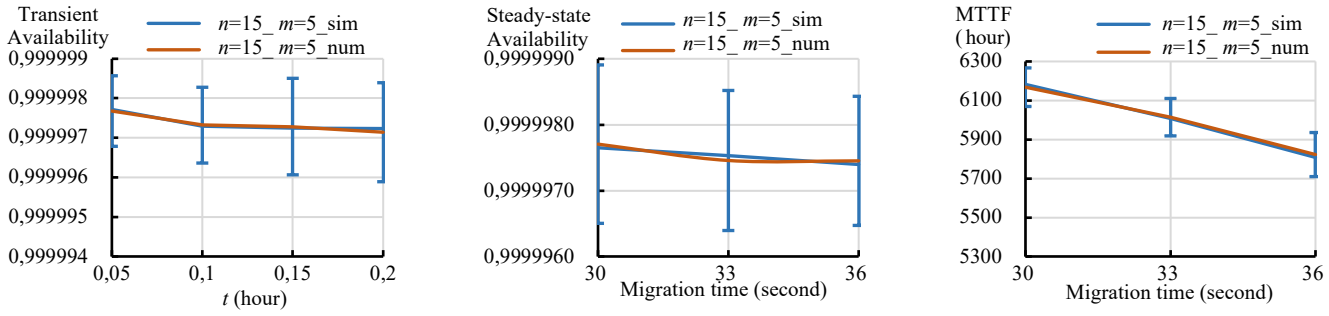

(a) Transient availability (b) Steady-state availability (c) MTTF

Fig. 5. Comparison of the numerical and the simulation results for each metric

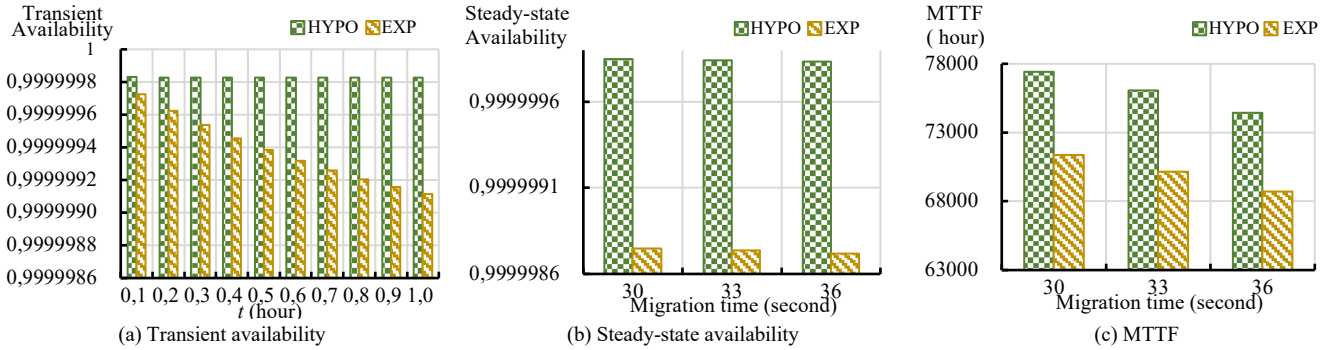

(a) Transient availability (b) Steady-state availability (c) MTTF

Fig. 6. Transient availability, steady-state availability and MTTF of a UMEC service chain under different failure time distributions

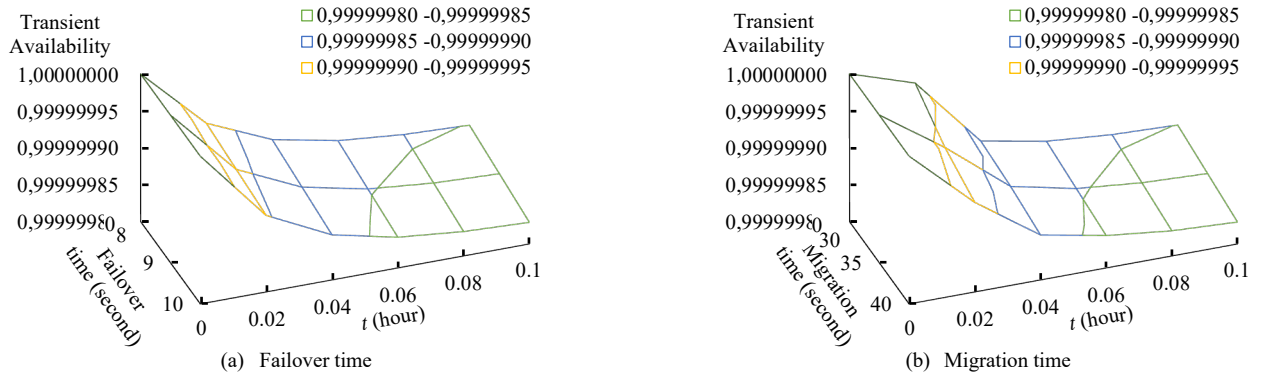

(a) Failover time (b) Migration time

Fig. 7. Transient availability of a UMEC service chain under different failover time and migration time

C. Sensitivity Analysis

This section presents the sensitivity analysis of MTTF, steady-state availability and transient availability of a UMEC service chain in regard to system parameters. Based on Equations (4) and (15), the scaled sensitivities $SS_{\omega}(\mathrm{A}_{TUM}(t))$ of transient availability can be calculated. Based on Equations (7) and (15), the scaled sensitivities $SS_{\omega}(\mathrm{A}_{SUM})$ of steady-state availability can be calculated. Based on Equations (14) and (15), the scaled sensitivities $SS_{\omega}(\mathrm{MTTF})$ of MTTF can be calculated. TABLE IV gives the numerical results of the scaled sensitivities of each metric in regard to system parameters, where '--' denotes that the corresponding metric is not affected by this parameter. The experimental results illustrate that the sensitivities of each metric with respect to λ_{o11}, λ_{o12}, λ_{v111} and λ_{v112} are negative, while the sensitivities of transient and steady-state availability in regard to the remaining parameters are positive, and the sensitivities of MTTF with respect to β_{v11} and γ_{o1} are positive. In addition, we can observe that γ_{o1} is a parameter significantly affecting the transient availability, steady-state availability and MTTF. Therefore, network service providers can improve the resilience of a UMEC service chain by adjusting the values of parameters that have a significant impact on the resilience.

$$SS_{\omega}(\mathrm{Y}) = \frac{\partial \mathrm{Y}}{\partial \omega}\left(\frac{\omega}{Y}\right) \tag{15}$$

TABLE III
Parameter Settings in the Simulation

Symbol	Default Values	Symbol	Default Values
T_{dvij}	3-4 days	T_{roi}	30-40 seconds
T_{doi}	7-8 days	T_{rbi}	1-1.5 minutes
T_{fvij}	1-2 days	T_{RV}	10-20 seconds
T_{foi}	5-6 days	T_{RO}	1-2 minutes
T_{rvij}	8-10 seconds	T_{R}	0.8-1.2 hours

TABLE IV
The Scaled Sensitivities for Each Metric

Parameter	$SS_{\omega}(A_{TUM}(0.05))$	$SS_{\omega}(A_{SUM})$	SS_{ω}(MTTF)
λ_{o11}	-6.55e-14	-1.99e-12	-1.50e-7
λ_{o12}	-6.55e-14	-1.99e-12	-1.50e-7
λ_{v111}	-2,31e-13	-5.19e-12	-3.92e-7
λ_{v112}	-2.31e-13	-5.19e-12	-3.92e-7
β_{v11}	3.52e-9	3.69e-9	5.06e-2
γ_{o1}	9.23e-9	1.30e-8	4.01e-2
δ_{1}	5.39e-10	7.53e-10	--
ε	3.25e-8	3.25e-8	--
φ	3.64e-8	7.36e-8	--
μ	7.24e-14	7.76e-11	--

D. Effect of Failure Time Distribution on Each Metric

This section presents the numerical results for MTTF, steady-state availability and transient availability of a UMEC service chain under different failure time distributions. We consider that failure time can follow a Hypoexponential distribution and an Exponential distribution. Fig. 4 (a) shows that when the migration rate is 90, the transient availability at t=0.1 is 0.999999829729 under failure time following the Hypoexponential distribution and 0.999999725690 under failure time following the Exponential distribution. Similar results are observed from Fig. 4 (b) and Fig. 4 (c), showing significant differences in the steady-state availability and the MTTF under failure time following the Hypoexponential distribution and the Exponential distribution. The reason is that the difference between the failure rates of these distributions is large. We can conclude that the type of failure time distribution has a significant impact on each metric studied.

E. Effect of System Parameters on Each Metric

This section first introduces the numerical results for MTTF, steady-state availability and transient availability of a UMEC service chain under different failover time, migration time, and numbers of VNFs and Primary UMEC Hosts. We then analyze the impact of time-varying parameters related to the resource degradation time, failure time and migration time on the transient availability of a UMEC service chain.

Fig. 5 shows the numerical results for the transient availability under different failover time and migration time. Fig. D-1 and Fig. D-2 in Appendix D of the supplementary file show the numerical results for the steady-state availability and MTTF of a UMEC service chain under different failover time and migration time, respectively. The numerical experiments illustrate that with increasing failover time and migration time, the resilience of a UMEC service chain gradually decreases. The reason is that the holding time of UMEC system remaining at the available states decreases while the probability of failure of the UMEC service chain increases with increasing failover time and migration time.

TABLE V shows the numerical results for MTTF, steady-state availability and transient availability of a UMEC service chain under different numbers of VNFs and Primary UMEC Hosts. We can observe that the resilience decreases with increasing number of VNFs, the availability decreases with decreasing number of Primary UMEC Hosts, and the reliability increases with decreasing number of Primary UMEC Hosts. The reason is that the number of components that can fail increases in the UMEC system due to increasing number of VNFs and Primary UMEC Hosts. However, the holding time of the system being available increases due to increasing number of Primary UMEC Hosts. Additionally, during VNF recovery, there is a higher probability that the resource degradation of other components will lead to the system being unavailable.

In addition, the position of UAV u and the position of user s can vary over time, which causes the resource degradation time, failure time and migration time to vary over time. Therefore, we can analyze the impact of UAV position change on the transient availability of a UMEC service chain by carrying out the numerical experiments of evaluating the effect of time-varying parameters, such as α_{o1}, λ_{o12} and γ_{o1} (defined in Section IV-A), related to the resource degradation time, failure time and migration time. Fig. 8 shows the numerical results of the transient availability with and without time-varying parameters. In this figure, yellow dots indicate the transient availability without time-varying parameters and blue, green and purple lines indicate the transient availability with time-varying α_{o1}, λ_{o12} and γ_{o1}, respectively. The aforementioned parameters are set to 0.0009, 0.0052 and 100 in defaults, respectively. Some explanations are as follows.

- At t=2 hours, as α_{o1} decreases, the transient availability increases compared to that without time-varying parameter.
- At t=3 hours, as γ_{o1} increases, the transient availability increases significantly compared to that without time-varying parameter.
- At t=4 hour, as α_{o1} increases, the transient availability decreases gradually and its value is less than that after 4 hours. As λ_{o12} decreases, there is no significant change in the transient availability compared to that without time-varying parameter.
- At t=5 hours, as γ_{o1} decreases, the transient availability decreases significantly and its value is lower than that without time-varying parameter.
- At t=6 hours, as α_{o1} decreases, the transient availability is greater than that without time-varying parameter.

These experimental results can help service providers provide availability-guaranteed UMEC service chain under UAV position change.

V. Discussion

This paper takes a first step towards quantitatively analyzing the resilience of a UMEC service chain consisting of any number of VNFs executed in any number of Primary UMEC Hosts. However, the limitation of our model is that we only analyze how the nodes (namely, Primary UMEC Hosts) executing VNFs affect the resilience of a UMEC service chain. In addition to Primary UMEC Hosts, there are three main nodes in the UMEC system: (i) GCS, which can provide appropriate resources and a stable environment for the operation of GCS software applications (such as MANO and the mission planner) [37]. (ii) Backup GCS, which can take over GCS software applications when the OS running these applications experiences resource degradation. And (iii) Backup UMEC Hosts, which can take over the processing requests when Primary UMEC Host OSes experience resource degradation.

Components in the aforementioned nodes can experience resource degradation and failure. The modeling approach proposed in Section III can be extended to model this case. Specifically, we develop a hierarchical model, composed of low-level model and high-level model, to capture the behaviors of components in the aforementioned nodes, while avoiding model largeness due to the complex interactions among components and model stiffness due to large differences in the abnormal event occurrence rate among components in the UMEC Hosts and GCS. We first adopt RBD to develop the low-level model, which can characterize the dependencies between UMEC hosts and GCS, shown in Fig. 9.

We then adopt SMP to develop the high-level model consists of two SMP models: (i) SMP model for capturing the behaviors of components (OS and VNF) in Primary and Backup UMEC Hosts, shown in Fig. 10 and (ii) SMP model for capturing the behaviors of components (OS and GCS software applications, such as MANO and the mission planner) in GCS and Backup GCS. The model under m=1 in Fig. 10 can be used as the SMP model for capturing the behaviors of components in GCS and Backup GCS.

Note that management and orchestration (MANO) consists of three components: NFV orchestrator (NFVO), VNF manager (VNFM), and virtual infrastructure manager (VIM). Without loss of generality, we consider that MANO is a single entity where the failure of any of its components will lead to MANO failure. TABLE VI gives the definition of variables used in the extended models. State *U* (Unknown) denotes that backup VNF (OS) is at one of Healthy, Resource Degradation and Failed states. State *BR* (Restart/Reboot Completion) denotes that backup VNF (OS) is at after the completion of restarting (rebooting). State *BP* (Repair Completion) denotes that backup VNF (OS) is at after the completion of repair and restarting (rebooting).

VI. Conclusion and Future Work

In this paper, we propose an SMP model for capturing the behaviors of a UMEC system that implements rejuvenation techniques. We derive the formulas to analyze the resilience of a UMEC service chain consisting of any number of VNFs executed in any number of Primary UMEC Hosts. Conducting numerical experiments, we quantitatively analyze the impact of type of failure time distribution and system parameters on the reliability, steady-state availability and transient availability of a UMEC service chain. In particular, we are able to identify potential bottlenecks for the resilience improvement, which can help design the UMEC service chain with high-grade resilience requirements and provide guidelines for system optimization.

In the UMEC system, there are three main components: MANO, NFV infrastructure (NFVI) and the mission planner [18]. The proposed model did not analyze the behaviors of NFVI. As future work, we will extend our model to evaluate the impact of NFVI on the resilience of a UMEC service chain. In addition, the numerical results in Section IV reveal that the availability increases with increasing number of UAVs. The UMEC service chain is deployed on multiple UAVs, which can meet the availability requirements, but lead to the increase in transmission delay between UAVs. Moreover, the transmission delay is affected by UAV position. Therefore, based on the closed-form solutions of calculating the resilience derived in this paper, we will design an optimization algorithm to ensure the trade-off between performance (such as end-to-end delay) and resilience, taking into account the positions of UAVs.

TABLE V
Transient Availability, Steady-state Availability and MTTF of a UMEC Service Chain under Different Numbers of VNFs and Primary UMEC Hosts

Numbers of VNFs and Primary UMEC Hosts	Steady-state Availability	MTTF	Transient Availability
n=15, m=5	0.999999838941	75436.89	0.999999860988
n=14, m=5	0.999999856454	84913.82	0.999999876332
n=13, m=5	0.999999871976	96333.61	0.999999889935
n=15, m=4	0.999999829671	80369.91	0.999999851021
n=15, m=3	0.999999815925	85687.41	0.999999835812

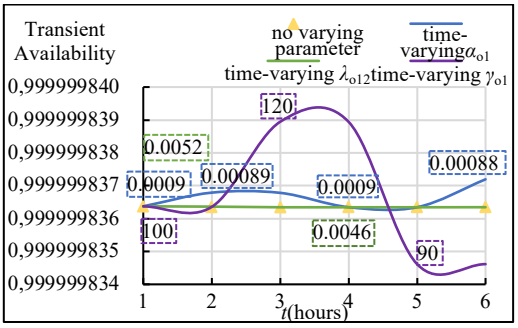

Fig. 8. Transient availability of a UMEC service chain with and without time-varying parameters

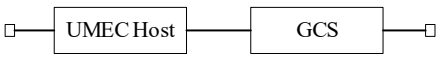

Fig. 9. RBD for the UMEC system

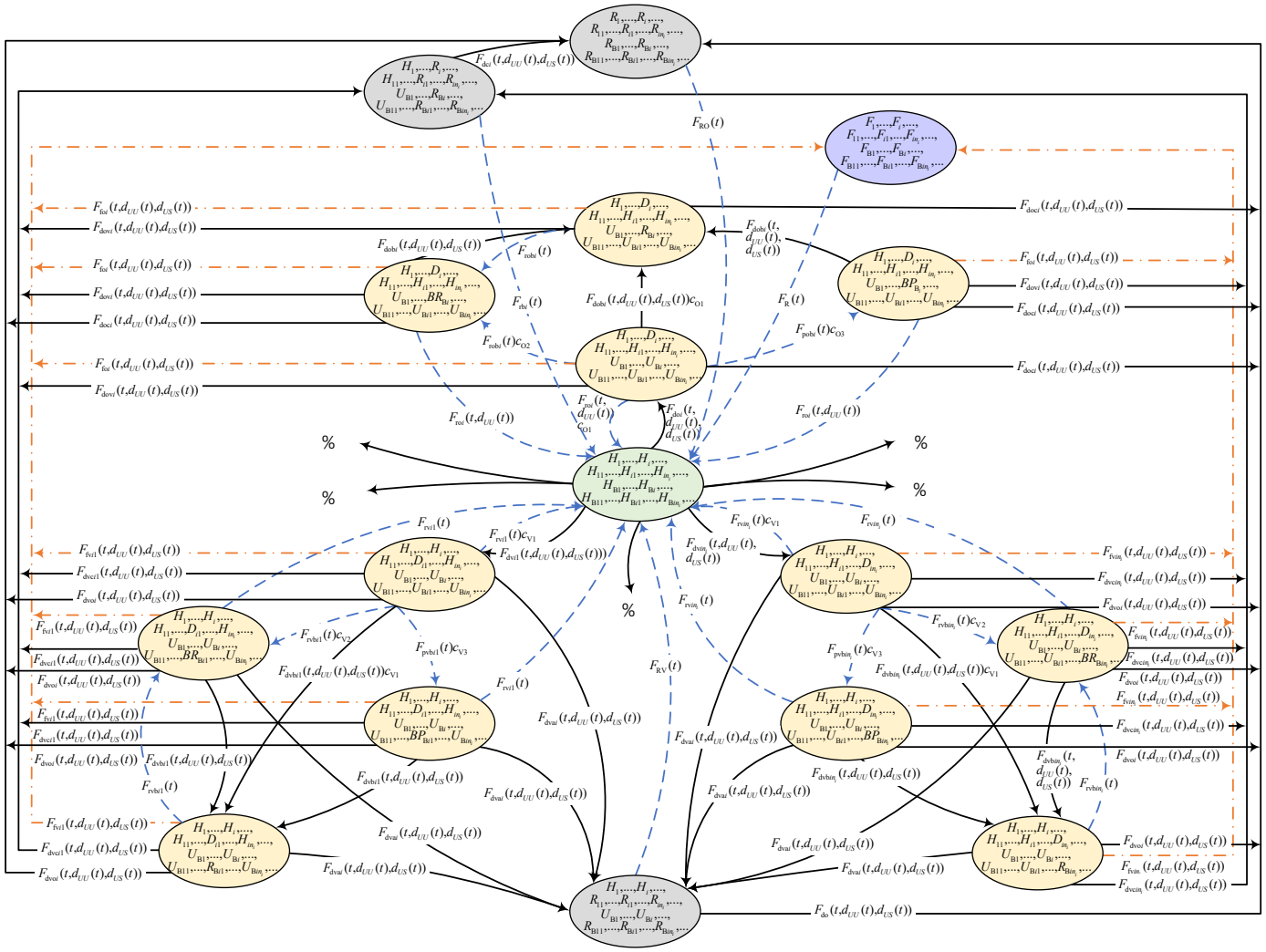

Fig. 10. SMP model for capturing the behaviors of components in Primary and Backup UMEC Hosts

TABLE VI
Definition of Variables Used in the Extended Model

Symbol	Definition
T_{dobi}	A random variable with CDF $F_{dobi}(t, d_{UU}(t), d_{US}(t))$ denoting the holding time of the i^{th} backup OS from *H*/*BR*/*BP* to *D*.
T_{dvbij}	A random variable with CDF $F_{dvbij}(t, d_{UU}(t), d_{US}(t))$ denoting the holding time of the j^{th} backup VNF running on the i^{th} OS from *H*/*BR*/*BP* to *D*.
T_{robi}	A random variable with CDF $F_{robi}(t)$ denoting the holding time of the i^{th} backup OS from *D* to *BR*.
T_{rvbij}	A random variable with CDF $F_{rvbij}(t)$ denoting the holding time of the j^{th} backup VNF running on the i^{th} OS from *D* to *BR*.
T_{pobi}	A random variable with CDF $F_{pobi}(t)$ denoting the holding time of the i^{th} backup OS from *D* to *BP*.
T_{pvbij}	A random variable with CDF $F_{pvbij}(t)$ denoting the holding time of the j^{th} backup VNF running on the i^{th} OS from *D* to *BP*.

ACKNOWLEDGMENTS

We would like to thank the editors and the anonymous reviewers very much for their insightful comments and suggestions that greatly improved the quality of this paper. The work of Jing Bai and Xiaolin Chang was supported in part by Beijing Municipal Natural Science Foundation (No. M22037). The research of Ricardo J. Rodríguez was supported in part by the University, Industry and Innovation Department of the Aragonese Government under Programa de Proyectos Estratégicos de Grupos de Investigación (DisCo research group, ref. T21-20R

REFERENCES

[1] Tiago Koketsu Rodrigues, Jiajia Liu, Nei Kato: Offloading Decision for Mobile Multi-Access Edge Computing in a Multi-Tiered 6G Network. IEEE Trans. Emerg. Top. Comput. (Early Access) (2021).
[2] Dario Sabella, Alessandro Vaillant, Pekka Kuure, Uwe Rauschenbach, Fabio Giust: Mobile-Edge Computing Architecture: The role of MEC in the Internet of Things. IEEE Consumer Electron. Mag. 5(4): 84-91 (2016).
[3] Tiago Koketsu Rodrigues, Katsuya Suto, Hiroki Nishiyama, Jiajia Liu, Nei Kato: Machine Learning Meets Computation and Communication

Control in Evolving Edge and Cloud: Challenges and Future Perspective. IEEE Commun. Surv. Tutorials 22(1): 38-67 (2020).
[4] Haotong Cao, Jianbo Du, Haitao Zhao, Daniel Xiapu Luo, Neeraj Kumar, Longxiang Yang, F. Richard Yu: Resource-Ability Assisted Service Function Chain Embedding and Scheduling for 6G Networks With Virtualization. IEEE Trans. Veh. Technol. 70(4): 3846-3859 (2021).
[5] Danyang Zheng, Evrim Guler, Chengzong Peng, Guangchun Luo, Ling Tian, Xiaojun Cao: Dependence-Aware Service Function Chain Embedding in Optical Networks. ICC 2019: 1-6.
[6] Bego Blanco, Jose Oscar Fajardo, Ioannis Giannoulakis, Emmanouil Kafetzakis, Shuping Peng, Jordi Pérez-Romero, Irena Trajkovska, Pouria Sayyad Khodashenas, Leonardo Goratti, Michele Paolino, Evangelos Sfakianakis, Fidel Liberal, George Xilouris: Technology pillars in the architecture of future 5G mobile networks: NFV, MEC and SDN. Comput. Stand. Interfaces 54: 216-228 (2017).
[7] Haibo Mei, Kun Yang, Qiang Liu, Kezhi Wang: Joint Trajectory-Resource Optimization in UAV-Enabled Edge-Cloud System With Virtualized Mobile Clone. IEEE Internet Things J. 7(7): 5906-5921 (2020).
[8] Yu Xu, Tiankui Zhang, Yuanwei Liu, Dingcheng Yang, Lin Xiao, Meixia Tao: UAV-Assisted MEC Networks with Aerial and Ground Cooperation. IEEE Trans. Wirel. Commun. (Early Access) (2021).
[9] Hichem Sedjelmaci, Sidi Mohammed Senouci, Nirwan Ansari: Intrusion Detection and Ejection Framework Against Lethal Attacks in UAV-Aided Networks: A Bayesian Game-Theoretic Methodology. IEEE Trans. Intell. Transp. Syst. 18(5): 1143-1153 (2017).
[10] Haixia Peng, Xuemin Sherman Shen: DDPG-based Resource Management for MEC/UAV-Assisted Vehicular Networks. VTC Fall 2020: 1-6.
[11] Qixun Zhang, Jingran Chen, Lei Ji, Zhiyong Feng, Zhu Han, Zhiyong Chen: Response Delay Optimization in Mobile Edge Computing Enabled UAV Swarm. IEEE Trans. Veh. Technol. 69(3): 3280-3295 (2020).
[12] Oussama Bekkouche, Konstantinos Samdanis, Miloud Bagaa, Tarik Taleb: A Service-Based Architecture for Enabling UAV Enhanced Network Services. IEEE Netw. 34(4): 328-335 (2020).
[13] Farheen Syed, Sachin Kumar Gupta, Saeed Hamood Alsamhi, Mamoon Rashid, Xuan Liu: A survey on recent optimal techniques for securing unmanned aerial vehicles applications. Trans. Emerg. Telecommun. Technol. 32(7) (2021).
[14] Kshira Sagar Sahoo, Sanjaya Kumar Panda, Sampa Sahoo, Bibhudatta Sahoo, Ratnakar Dash: Toward secure software-defined networks against distributed denial of service attack. J. Supercomput. 75(8): 4829-4874 (2019).
[15] Gregory Levitin, Liudong Xing, Yanping Xiang: Optimizing software rejuvenation policy for tasks with periodic inspections and time limitation. Reliab. Eng. Syst. Saf. 197: 106776 (2020).
[16] Chafika Benzaid, Tarik Taleb: AI-Driven Zero Touch Network and Service Management in 5G and Beyond: Challenges and Research Directions. IEEE Netw. 34(2): 186-194 (2020).
[17] Kishor S. Trivedi, Andrea Bobbio: Reliability and Availability: Modeling, Analysis, Application. Cambridge University Press, 2017.
[18] OSM, OSM PoC 10 Automated Deployment of an IP Telephony Service on UAVs using OSM. [Online]. Available: https://osm.etsi.org/wikipub/index.php/OSM_PoC_10_Automated_Deployment_of_an_IP_Telephony_Service_on_UAVs_using_OSM.
[19] Mushu Li, Nan Cheng, Jie Gao, Yinlu Wang, Lian Zhao, Xuemin Shen: Energy-Efficient UAV-Assisted Mobile Edge Computing: Resource Allocation and Trajectory Optimization. IEEE Trans. Veh. Technol. 69(3): 3424-3438 (2020).
[20] Jiao Zhang, Li Zhou, Fuhui Zhou, Boon-Chong Seet, Haijun Zhang, Zhiping Cai, Jibo Wei: Computation-Efficient Offloading and Trajectory Scheduling for Multi-UAV Assisted Mobile Edge Computing. IEEE Trans. Veh. Technol. 69(2): 2114-2125 (2020).
[21] Kaiyuan Zhang, Xiaolin Gui, Dewang Ren, Defu Li: Energy-Latency Tradeoff for Computation Offloading in UAV-Assisted Multiaccess Edge Computing System. IEEE Internet Things J. 8(8): 6709-6719 (2021).
[22] Hongyue Kang, Xiaolin Chang, Jelena Mišić, Vojislav B. Mišić, Junchao Fan: Joint Optimization of UAV Trajectory and Task Scheduling in SAGIN: Delay Driven. ICSOC 2021.
[23] Guanghan Bai, Yanjun Li, Yining Fang, Yun-An Zhang, Junyong Tao: Network approach for resilience evaluation of a UAV swarm by considering communication limits. Reliab. Eng. Syst. Saf. 193: 106602 (2020).
[24] Long Qu, Maurice Khabbaz, Chadi Assi: Reliability-Aware Service Chaining In Carrier-Grade Softwarized Networks. IEEE J. Sel. Areas Commun. 36(3): 558-573 (2018).
[25] Anna Engelmann, Admela Jukan: A Reliability Study of Parallelized VNF Chaining. ICC 2018: 1-6.
[26] Matheus Torquato, Paulo R. M. Maciel, Marco Vieira: Availability and reliability modeling of VM migration as rejuvenation on a system under varying workload. Softw. Qual. J. 28(1): 59-83 (2020).
[27] Besmir Tola, Gianfranco Nencioni, Bjarne E. Helvik: Network-Aware Availability Modeling of an End-to-End NFV-Enabled Service. IEEE Trans. Netw. Serv. Manag. 16(4): 1389-1403 (2019).
[28] Mario Di Mauro, Giovanni Galatro, Fabio Postiglione, Marco Tambasco: Performability of Network Service Chains: Stochastic Modeling and Assessment of Softwarized IP Multimedia Subsystem. IEEE Trans. Dependable Secur. Comput. (Early Access) (2021).
[29] Fumio Machida, Jianwen Xiang, Kumiko Tadano, Yoshiharu Maeno: Lifetime Extension of Software Execution Subject to Aging. IEEE Trans. Reliab. 66(1): 123-134 (2017).
[30] Jing Bai, Xiaolin Chang, Gaorong Ning, Zhenjiang Zhang, Kishor S. Trivedi: Service Availability Analysis in a Virtualized System: A Markov Regenerative Model Approach. IEEE Trans. Cloud Comput. (Early Access) (2020).
[31] Jing Bai, Xiaolin Chang, Kishor S. Trivedi, Zhen Han: Resilience-Driven Dependability and Security Analysis of Vehicle Platooning Services. IEEE Trans. Veh. Technol.70(6): 5378-5389 (2020).
[32] Jing Bai, Xiaolin Chang, Fumio Machida, Lili Jiang, Zhen Han, Kishor S. Trivedi: Impact of Service Function Aging on the Dependability for MEC Service Function Chain. IEEE Trans. Dependable Secur. Comput. (Early Access) (2022).
[33] Javad Sabzehali, Vijay K. Shah, Qiang Fan, Biplav Choudhury, Lingjia Liu, Jeffrey H. Reed: Optimizing Number, Placement, and Backhaul Connectivity of Multi-UAV Networks. IEEE Internet of Things Journal. (Early Access) (2021).
[34] An Liu, Vincent K. N. Lau: Optimization of Multi-UAV-Aided Wireless Networking Over a Ray-Tracing Channel Model. IEEE Trans. Wirel. Commun. 18(9): 4518-4530 (2019).
[35] Besmir Tola, Yuming Jiang, Bjarne E. Helvik: Model-Driven Availability Assessment of the NFV-MANO With Software Rejuvenation. IEEE Trans. Netw. Serv. Manag. 18(3): 2460-2477 (2021).
[36] Maplesoft, Inc., Maple 18, http://www.maplesoft.com/products/maple.
[37] Aicha Idriss Hentati, Lobna Krichen, Mohamed Fourati and Lamia Chaari Fourati: Simulation Tools, Environments and Frameworks for UAV Systems Performance Analysis. IWCMC 2018.

Jing Bai is currently a Ph.D student at School of Computer and Information Technology, Beijing Jiaotong University. Her interests include software reliability and availability.

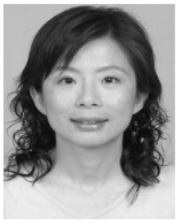

Xiaolin Chang is a professor at School of Computer and Information Technology, Beijing Jiaotong University. Her current research interests include blockchain, network security, secure and dependable machine learning. She is a senior member of IEEE.

Ricardo J. Rodríguez received the M.S. and Ph.D. degrees in computer science from the University of Zaragoza, Zaragoza, Spain, in 2010 and 2013, respectively, where his Ph.D. dissertation was focused on performance analysis and resource optimization in critical systems, with special interest in Petri net modeling techniques. He is currently an Assistant Professor at the Universidad de Zaragoza. His research interests include performability and dependability analysis, program binary analysis, and contactless cards security.

Kishor S. Trivedi holds the Hudson chair in the Department of Electrical and Computer Engineering at Duke University. He is the author of Probability and Statistics with Reliability, Queuing and Computer Science Applications, published by John Wiley. He has published more than 500 articles and has supervised more than 45 PhD dissertations. He received the IEEE Computer Society Technical Achievement Award for his research on software aging and rejuvenation.

Shupan Li is currently a lecturer in School of Information Engineering of Zhengzhou University, Zhengzhou, China. His current research interests include Industrial Internet, secure and Integrity verification.

Towards UAV-based MEC Service Chain Resilience Evaluation: A Quantitative Modeling Approach Supplementary File

Jing Bai, Xiaolin Chang, Ricardo J. Rodríguez, Kishor S. Trivedi, Shupan Li

APPENDIX A FORMULAS FOR CALCULATING TRANSIENT AVAILABILITY

This section gives the detailed process for calculating the transient availability of a unmanned aerial vehicle-based multi-access edge computing (UMEC) service chain mentioned in Section III-*B* of the main paper. The details are as follows.

The non-null elements of $\mathbf{K}_{UM}(t)$ are defined as $k_{ij}(t)=P\{X_{q+1}=j,T_{q+1}-T_q\le t \mid X_q=i\}$ and given by Equations (A.1)-(A.17),

$$k_{0(m+3+i)}(t)=\int_0^t \prod_{u\in A_i}(1-F_{\mathrm{do}u}(t,d_{UU}(t),d_{US}(t)))\prod_{r=1}^{m}\prod_{w=1}^{n_r}(1-F_{\mathrm{dv}rw}(t,d_{UU}(t),d_{US}(t)))dF_{\mathrm{do}i}(t,d_{UU}(t),d_{US}(t)) \tag{A.1}$$

$$k_{0(2m+3+\sum_{q=0}^{i-1}n_q+j)}(t)=\int_0^t \prod_{r=1}^{m}(1-F_{\mathrm{do}r}(t,d_{UU}(t),d_{US}(t)))\prod_{v\in B_{ij}}(1-F_{\mathrm{dv}iv}(t,d_{UU}(t),d_{US}(t)))\prod_{u\in A_i}\prod_{w=1}^{n_u}(1-F_{\mathrm{dv}uw}(t,d_{UU}(t),d_{US}(t)))dF_{\mathrm{dv}ij}(t,d_{UU}(t),d_{US}(t)) \tag{A.2}$$

$$k_{10}(t)=F_{\mathrm{R}}(t) \tag{A.3}$$

$$k_{20}(t)=F_{\mathrm{RO}}(t) \tag{A.4}$$

$$k_{30}(t)=\int_0^t(1-F_{\mathrm{do}}(t,d_{UU}(t),d_{US}(t)))dF_{\mathrm{RV}}(t) \tag{A.5}$$

$$k_{32}(t)=\int_0^t(1-F_{\mathrm{RV}}(t))dF_{\mathrm{do}}(t,d_{UU}(t),d_{US}(t)) \tag{A.6}$$

$$k_{(3+i)0}(t)=\int_0^t(1-F_{\mathrm{dc}i}(t,d_{UU}(t),d_{US}(t)))dF_{\mathrm{rb}i}(t) \tag{A.7}$$

$$k_{(3+i)2}(t)=\int_0^t(1-F_{\mathrm{rb}i}(t))dF_{\mathrm{dc}i}(t,d_{UU}(t),d_{US}(t)) \tag{A.8}$$

$$k_{(m+3+i)0}(t)=\int_0^t(1-F_{\mathrm{fo}i}(t,d_{UU}(t),d_{US}(t)))(1-F_{\mathrm{dov}i}(t,d_{UU}(t),d_{US}(t)))(1-F_{\mathrm{doc}i}(t,d_{UU}(t),d_{US}(t)))dF_{\mathrm{ro}i}(t,d_{UU}(t)) \tag{A.9}$$

$$k_{(m+3+i)1}(t)=\int_0^t(1-F_{\mathrm{ro}i}(t,d_{UU}(t)))(1-F_{\mathrm{dov}i}(t,d_{UU}(t),d_{US}(t)))(1-F_{\mathrm{doc}i}(t,d_{UU}(t),d_{US}(t)))dF_{\mathrm{fo}i}(t,d_{UU}(t),d_{US}(t)) \tag{A.10}$$

$$k_{(m+3+i)2}(t)=\int_0^t(1-F_{\mathrm{fo}i}(t,d_{UU}(t),d_{US}(t)))(1-F_{\mathrm{ro}i}(t,d_{UU}(t)))(1-F_{\mathrm{dov}i}(t,d_{UU}(t),d_{US}(t)))dF_{\mathrm{doc}i}(t,d_{UU}(t),d_{US}(t)) \tag{A.11}$$

$$k_{(m+3+i)(i+3)}(t)=\int_0^t(1-F_{\mathrm{fo}i}(t,d_{UU}(t),d_{US}(t)))(1-F_{\mathrm{ro}i}(t,d_{UU}(t)))(1-F_{\mathrm{doc}i}(t,d_{UU}(t),d_{US}(t)))dF_{\mathrm{dov}i}(t,d_{UU}(t),d_{US}(t)) \tag{A.12}$$

$$k_{(2m+3+\sum_{q=0}^{i-1}n_q+j)0}(t)=\int_0^t(1-F_{\mathrm{fv}ij}(t,d_{UU}(t),d_{US}(t)))(1-F_{\mathrm{dvo}i}(t,d_{UU}(t),d_{US}(t)))(1-F_{\mathrm{dva}i}(t,d_{UU}(t),d_{US}(t)))(1-F_{\mathrm{dvc}ij}(t,d_{UU}(t),d_{US}(t)))dF_{\mathrm{rv}ij}(t) \tag{A.13}$$

$$k_{(2m+3+\sum_{q=0}^{i-1}n_q+j)1}(t)=\int_0^t(1-F_{\mathrm{dvo}i}(t,d_{UU}(t),d_{US}(t)))(1-F_{\mathrm{dva}i}(t,d_{UU}(t),d_{US}(t)))(1-F_{\mathrm{dvc}ij}(t,d_{UU}(t),d_{US}(t)))(1-F_{\mathrm{rv}ij}(t))dF_{\mathrm{fv}ij}(t,d_{UU}(t),d_{US}(t)) \tag{A.14}$$

$$k_{(2m+3+\sum_{q=0}^{i-1}n_q+j)2}(t)=\int_0^t(1-F_{\mathrm{fv}ij}(t,d_{UU}(t),d_{US}(t)))(1-F_{\mathrm{dvc}ij}(t,d_{UU}(t),d_{US}(t)))(1-F_{\mathrm{dva}i}(t,d_{UU}(t),d_{US}(t)))(1-F_{\mathrm{rv}ij}(t))dF_{\mathrm{dvo}i}(t,d_{UU}(t),d_{US}(t)) \tag{A.15}$$

$$k_{(2m+3+\sum_{q=0}^{i-1}n_q+j)3}(t)=\int_0^t(1-F_{\mathrm{fv}ij}(t,d_{UU}(t),d_{US}(t)))(1-F_{\mathrm{dvo}i}(t,d_{UU}(t),d_{US}(t)))(1-F_{\mathrm{dvc}ij}(t,d_{UU}(t),d_{US}(t)))(1-F_{\mathrm{rv}ij}(t))dF_{\mathrm{dva}i}(t,d_{UU}(t),d_{US}(t)) \tag{A.16}$$

- Jing Bai and Xiaolin Chang are with Beijing Key Laboratory of Security and Privacy in Intelligent Transportation, Beijing Jiaotong University, China. E-mail: {19112047, xlchang}@ bjtu.edu.cn. Xiaolin Chang is the corresponding author.
- Ricardo J. Rodríguez is with Departamento de Informática e Ingeniería de sistemas, Universidad de Zaragoza, Zaragoza, Spain. E-mail: rjrodriguez@unizar.es.
- Kishor S. Trivedi is with Department of Electrical and Computer Engineering, Duke University. E-mail: ktrivedi@duke.edu.
- Shupan Li is with School of Information Engineering, Zhengzhou University, Zhengzhou, China. E-mail: iespli@zzu.edu.cn.

$$k_{(2m+3+\sum_{q=0}^{i-1}n_q+j)(i+3)}(t)$$
$$=\int_0^t(1-F_{\mathrm{fv}ij}(t,d_{UU}(t),d_{US}(t)))(1-F_{\mathrm{dvo}i}(t,d_{UU}(t),d_{US}(t))) \quad (A.17)$$
$$(1-F_{\mathrm{dva}i}(t,d_{UU}(t),d_{US}(t)))(1-F_{\mathrm{rv}ij}(t))$$
$$dF_{\mathrm{dvc}ij}(t,d_{UU}(t),d_{US}(t))$$

where $1\le i\le m,\quad 1\le j\le n_i,\quad A_i=\{u\,|\,1\le u\le m,u\ne i\}$ and $B_{ij}=\{v\,|\,1\le v\le n_i,v\ne j\}$.

The unconditional probabilities for each system state are given in Equations (A.18)-(A.21),

$$\pi_1(t)=L^{-1}(-E_{11}^{\sim}(t)\sum_{i=m+4}^{2m+n+3}k_{0i}^{\sim}(t)k_{i1}^{\sim}(t)\Big/W) \quad (A.18)$$

$$\pi_2(t)$$
$$=L^{-1}(-E_{22}^{\sim}(t)(\sum_{i=2m+4}^{2m+n+3}k_{0i}^{\sim}(t)k_{i3}^{\sim}(t)k_{32}^{\sim}(t)$$
$$+\sum_{i=1}^{m}\sum_{j=1}^{n_i}k_{0(2m+3+\sum_{q=0}^{i-1}n_q+j)}^{\sim}(t)k_{(i+3)2}^{\sim}(t)k_{(2m+3+\sum_{q=0}^{i-1}n_q+j)(i+3)}^{\sim}(t) \quad (A.19)$$
$$+\sum_{i=m+4}^{2m+3}k_{0i}^{\sim}(t)k_{i(i-m)}^{\sim}(t)k_{(i-m)2}^{\sim}(t)+\sum_{i=m+4}^{2m+n+3}k_{0i}^{\sim}(t)k_{i2}^{\sim}(t))\Big/W)$$

$$\pi_3(t)=L^{-1}(-E_{33}^{\sim}(t)\sum_{i=2m+4}^{2m+n+3}k_{0i}^{\sim}(t)k_{i3}^{\sim}(t)\Big/W) \quad (A.20)$$

$$\pi_{(i+3)}(t)$$
$$=L^{-1}(-E_{(i+3)(i+3)}^{\sim}(t)(k_{0(i+3+m)}^{\sim}(t)k_{(i+3+j)(i+3)}(t) \quad (A.21)$$
$$+\sum_{j=1}^{n_i}k_{0(2m+3+\sum_{q=0}^{i-1}n_q+j)}^{\sim}(t)\,k_{(2m+3+\sum_{q=0}^{i-1}n_q+j)(i+3)}^{\sim}(t))\Big/W)$$

where $W=-1+\sum_{i=2m+4}^{2m+n+3}(k_{0i}^{\sim}(t)\;\;k_{i3}^{\sim}(t)\,(k_{30}^{\sim}(t)+k_{32}^{\sim}(t)\,k_{20}^{\sim}(t)))$

$$+\sum_{i=m+4}^{2m+3}(k_{0i}^{\sim}(t)k_{i(i-m)}^{\sim}(t)(k_{(i-m)0}^{\sim}(t)+k_{(i-m)2}^{\sim}(t)k_{20}^{\sim}(t)))+\sum_{i=m+4}^{2m+n+3}(k_{0i}^{\sim}(t)$$
$$(k_{i0}^{\sim}(t)+k_{i1}^{\sim}(t)k_{10}^{\sim}(t)+k_{i2}^{\sim}(t)\,k_{20}^{\sim}(t)))+\sum_{i=1}^{m}\sum_{j=1}^{n_i}(k_{0(2m+3+\sum_{q=0}^{i-1}n_q+j)}^{\sim}(t)$$
$$k_{(2m+3+\sum_{q=0}^{i-1}n_q+j)(i+3)}^{\sim}(t)(k_{(i+3)0}^{\sim}(t)+k_{(i+3)2}^{\sim}(t)k_{20}^{\sim}(t))),\ 1\le i\le m$$ and $k_{ij}^{\sim}(t)$ can be obtained by applying Equations (A.1)-(A.17).

APPENDIX B FORMULAS FOR CALCULATING STEADY-STATE AVAILABILITY

This section gives the detailed process of calculating the steady-state availability of a UMEC service chain mentioned in Section III-*C* of the main paper. The details are as follows.

The steady-state probabilities of the embedded discrete time Markov chain (DTMC) at each system state are given in Equations (B.1)-(B.6),

$$V_2^*$$
$$=(\sum_{i=m+4}^{2m+n+3}p_{0i}p_{i2}+\sum_{i=2m+4}^{2m+n+3}p_{0i}p_{i3}p_{32}+\sum_{i=1}^{m}\sum_{j=1}^{n_i}p_{0(2m+3+\sum_{q=0}^{i-1}n_q+j)} \quad (B.1)$$
$$p_{(2m+3+\sum_{q=0}^{i-1}n_q+j)(i+3)}p_{(i+3)2}+\sum_{i=4}^{m+3}p_{0(i+m)}p_{(i+m)i}p_{i2})\Big/M$$

$$V_{(i+3)}^*$$
$$=(\sum_{j=1}^{n_i}(p_{0(2m+3+\sum_{q=0}^{i-1}n_q+j)}p_{(2m+3+\sum_{q=0}^{i-1}n_q+j)(i+3)})+p_{0(i+3+m)} \quad (B.2)$$
$$p_{(i+3+m)(i+3)})\Big/M$$

$$V_3^*=\sum_{i=2m+4}^{2m+n+3}p_{0i}p_{i3}\Big/M \quad (B.3)$$

$$V_1^*=\sum_{i=m+4}^{2m+n+3}p_{0i}p_{i1}\Big/M \quad (B.4)$$

$$V_{(m+3+g)}^*=p_{0(m+3+g)}\Big/M \quad (B.5)$$

$$V_0^*=1/M \quad (B.6)$$

where $M=\sum_{i=4}^{m+3}(p_{0(i+m)}p_{(i+m)i}(1+p_{i2}))+1+\sum_{i=1}^{m}\sum_{j=1}^{n_i}\Big((1+p_{(i+3)2})$
$p_{0(2m+3+\sum_{q=0}^{i-1}n_q+j)}p_{(2m+3+\sum_{q=0}^{i-1}n_q+j)(i+3)}\Big)+\sum_{i=m+4}^{2m+n+3}(p_{0i}p_{i1}+p_{0i}p_{i2}+p_{0i})$
$+\sum_{i=2m+4}^{2m+n+3}(p_{0i}p_{i3}p_{32}+p_{0i}p_{i3}),\quad 1\le i\le m$ and $1\le g\le m+n$.

The mean sojourn times at each system state are given in Equations (B.7)-(B.13).

$$h_{(2m+3+\sum_{q=0}^{i-1}n_q+j)}^*$$
$$=\int_0^\infty(1-F_{\mathrm{fv}ij}(t,d_{UU}(t),d_{US}(t)))(1-F_{\mathrm{dvc}ij}(t,d_{UU}(t),d_{US}(t))) \quad (B.7)$$
$$(1-F_{\mathrm{dva}i}(t,d_{UU}(t),d_{US}(t)))(1-F_{\mathrm{rv}ij}(t))(1$$
$$-F_{\mathrm{dvo}i}(t,d_{UU}(t),d_{US}(t)))dt$$

$$h_{(m+3+i)}^*$$
$$=\int_0^\infty(1-F_{\mathrm{fo}i}(t,d_{UU}(t),d_{US}(t)))(1-F_{\mathrm{ro}i}(t,d_{UU}(t)))(1 \quad (B.8)$$
$$-F_{\mathrm{dov}i}(t,d_{UU}(t),d_{US}(t)))(1-F_{\mathrm{doc}i}(t,d_{UU}(t),d_{US}(t)))dt$$

$$h_0^*$$
$$=\int_0^\infty\prod_{i=1}^{m}(1-F_{\mathrm{do}i}(t,d_{UU}(t),d_{US}(t)))\prod_{i=1}^{m}\prod_{j=1}^{n_i}(1-F_{\mathrm{dv}ij}(t, \quad (B.9)$$
$$d_{UU}(t),d_{US}(t)))dt$$

$$h_{(3+i)}^*=\int_0^\infty(1-F_{\mathrm{dc}i}(t,d_{UU}(t),d_{US}(t)))(1-F_{\mathrm{rb}i}(t))dt \quad (B.10)$$

$$h_3^*=\int_0^\infty(1-F_{\mathrm{do}}(t,d_{UU}(t),d_{US}(t)))(1-F_{\mathrm{RV}}(t))dt \quad (B.11)$$

$$h_2^*=\int_0^\infty(1-F_{\mathrm{RO}}(t))dt \quad (B.12)$$

$$h_1^*=\int_0^\infty(1-F_{\mathrm{R}}(t))dt \quad (B.13)$$

where $1\le i\le m$ and $1\le j\le n_i$.

APPENDIX C FORMULAS FOR CALCULATING MTTF

This section gives the detailed process of calculating MTTF (the mean time to failure) of a UMEC service chain

mentioned in Section III-*D*. The non-null parameters in $\mathbf{P}'_{UM}$ are given in Equations (C.1)-(C.16),

$$p'_{0i} = \int_0^\infty \prod_{u\in A_i}(1-F_{\mathrm{dou}}(t,d_{UU}(t),d_{US}(t)))\prod_{r=1}^{m}\prod_{j=1}^{n_r}(1-F_{\mathrm{dvrj}}(t, d_{UU}(t),d_{US}(t)))dF_{\mathrm{doi}}(t,d_{UU}(t),d_{US}(t)) \quad (C.1)$$

$$p'_{0(m+\sum_{q=0}^{i-1}n_q+j)} = \int_0^\infty \prod_{r=1}^{m}(1-F_{\mathrm{dor}}(t,d_{UU}(t),d_{US}(t)))\prod_{v\in B_{ij}}(1-F_{\mathrm{dviv}}(t,d_{UU}(t), d_{US}(t)))\prod_{u\in A_i}\prod_{w=1}^{n_u}(1-F_{\mathrm{dvuw}}(t,d_{UU}(t),d_{US}(t)))dF_{\mathrm{dvij}}(t,d_{UU}(t),d_{US}(t)) \quad (C.2)$$

$$p'_{i0} = \int_0^\infty (1-F_{\mathrm{foi}}(t,d_{UU}(t),d_{US}(t)))(1-F_{\mathrm{dovi}}(t,d_{UU}(t), d_{US}(t)))(1-F_{\mathrm{doci}}(t,d_{UU}(t),d_{US}(t)))dF_{\mathrm{roi}}(t,d_{UU}(t)) \quad (C.3)$$

$$p'_{i(2m+n+1)} = \int_0^\infty (1-F_{\mathrm{roi}}(t,d_{UU}(t)))(1-F_{\mathrm{dovi}}(t,d_{UU}(t),d_{US}(t)))(1-F_{\mathrm{doci}}(t,d_{UU}(t),d_{US}(t)))dF_{\mathrm{foi}}(t,d_{UU}(t),d_{US}(t)) \quad (C.4)$$

$$p'_{i(2m+n+2)} = \int_0^\infty (1-F_{\mathrm{foi}}(t,d_{UU}(t),d_{US}(t)))(1-F_{\mathrm{roi}}(t,d_{UU}(t)))(1-F_{\mathrm{dovi}}(t,d_{UU}(t),d_{US}(t)))dF_{\mathrm{doci}}(t,d_{UU}(t),d_{US}(t)) \quad (C.5)$$

$$p'_{i(m+n+i)} = \int_0^\infty (1-F_{\mathrm{foi}}(t,d_{UU}(t),d_{US}(t)))(1-F_{\mathrm{roi}}(t,d_{UU}(t)))(1-F_{\mathrm{doci}}(t,d_{UU}(t),d_{US}(t)))dF_{\mathrm{dovi}}(t,d_{UU}(t),d_{US}(t)) \quad (C.6)$$

$$p'_{(m+\sum_{q=1}^{i-1}n_q+j)0} = \int_0^\infty (1-F_{\mathrm{fvij}}(t,d_{UU}(t),d_{US}(t)))(1-F_{\mathrm{dvoi}}(t,d_{UU}(t),d_{US}(t)))(1-F_{\mathrm{dvai}}(t,d_{UU}(t),d_{US}(t)))(1-F_{\mathrm{dvcij}}(t,d_{UU}(t),d_{US}(t)))dF_{\mathrm{rvij}}(t) \quad (C.7)$$

$$p'_{(m+\sum_{q=1}^{i-1}n_q+j)(2m+n+1)} = \int_0^\infty (1-F_{\mathrm{dvoi}}(t,d_{UU}(t),d_{US}(t)))(1-F_{\mathrm{dvai}}(t,d_{UU}(t),d_{US}(t)))(1-F_{\mathrm{dvcij}}(t,d_{UU}(t),d_{US}(t)))(1-F_{\mathrm{rvij}}(t))dF_{\mathrm{fvij}}(t,d_{UU}(t),d_{US}(t)) \quad (C.8)$$

$$p'_{(m+\sum_{q=1}^{i-1}n_q+j)(2m+n+2)} = \int_0^\infty (1-F_{\mathrm{fvij}}(t,d_{UU}(t),d_{US}(t)))(1-F_{\mathrm{dvcij}}(t,d_{UU}(t),d_{US}(t)))(1-F_{\mathrm{dvai}}(t,d_{UU}(t),d_{US}(t)))(1-F_{\mathrm{rvij}}(t))dF_{\mathrm{dvoi}}(t,d_{UU}(t),d_{US}(t)) \quad (C.9)$$

$$p'_{(m+\sum_{q=1}^{i-1}n_q+j)(2m+n+3)} = \int_0^\infty (1-F_{\mathrm{fvij}}(t,d_{UU}(t),d_{US}(t)))(1-F_{\mathrm{dvoi}}(t,d_{UU}(t),d_{US}(t)))(1-F_{\mathrm{dvcij}}(t,d_{UU}(t),d_{US}(t)))(1-F_{\mathrm{rvij}}(t))dF_{\mathrm{dvai}}(t,d_{UU}(t),d_{US}(t)) \quad (C.10)$$

$$p'_{(m+\sum_{q=0}^{i-1}n_q+j)(m+n+i)} = \int_0^\infty (1-F_{\mathrm{fvij}}(t,d_{UU}(t),d_{US}(t)))(1-F_{\mathrm{dvoi}}(t,d_{UU}(t),d_{US}(t)))(1-F_{\mathrm{dovij}}(t,d_{UU}(t),d_{US}(t)))(1-F_{\mathrm{rvij}}(t))dF_{\mathrm{dvcij}}(t,d_{UU}(t),d_{US}(t)) \quad (C.11)$$

$$p'_{(m+n+i)(m+n+i)} = 1 \quad (C.12)$$

$$p'_{(2m+n+1)(2m+n+1)} = 1 \quad (C.14)$$

$$p'_{(2m+n+2)(2m+n+2)} = 1 \quad (C.15)$$

$$p'_{(2m+n+3)(2m+n+3)} = 1 \quad (C.16)$$

where $1 \le i \le m$ and $1 \le j \le n_i$.

APPENDIX D NUMERICAL RESULTS

This section introduces the numerical results for the steady-state availability and MTTF of a UMEC service chain under different failover time and migration time, shown in Fig. D-1 and Fig. D-2.

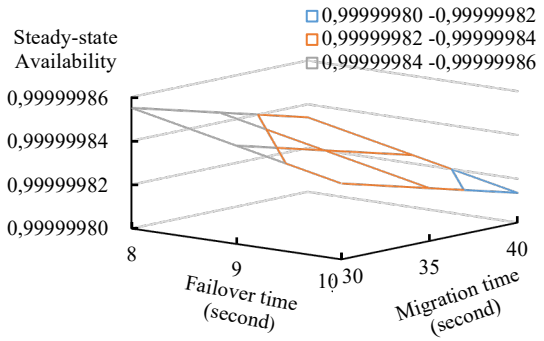

Fig. D-1. Steady-state availability of a UMEC service chain under different failover time and migration time

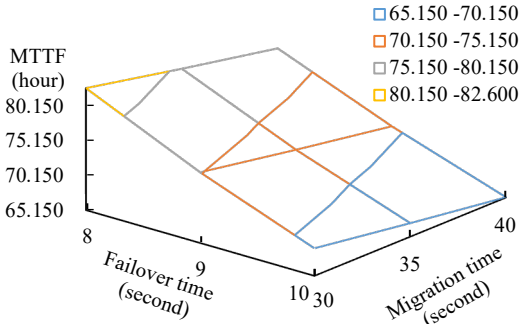

Fig. D-2. MTTF of a UMEC service chain under different failover time and migration time